LASER INTERFEROMETER GRAVITATIONAL WAVE OBSERVATORY
- LIGO -
CALIFORNIA INSTITUTE OF TECHNOLOGY
MASSACHUSETTS INSTITUTE OF TECHNOLOGY

Technical Note **LIGO-T1500346–v2** 2015/10/29

Excessive Noise in High current Photodetection

Project Report- SURF 2015

Arjun Iyer, Zach Korth, Eric Gustafson, Rana Adhikari

California Institute of Technology
LIGO Project, MS 18-34
Pasadena, CA 91125
Phone (626) 395-2129
Fax (626) 304-9834
E-mail: info@ligo.caltech.edu

Massachusetts Institute of Technology
LIGO Project, Room NW22-295
Cambridge, MA 02139
Phone (617) 253-4824
Fax (617) 253-7014
E-mail: info@ligo.mit.edu

LIGO Hanford Observatory
Route 10, Mile Marker 2
Richland, WA 99352
Phone (509) 372-8106
Fax (509) 372-8137
E-mail: info@ligo.caltech.edu

LIGO Livingston Observatory
19100 LIGO Lane
Livingston, LA 70754
Phone (225) 686-3100
Fax (225) 686-7189
E-mail: info@ligo.caltech.edu

http://www.ligo.caltech.edu/

Contents

List of Figures

Acknowledgment

I would like start by thanking the NSF and Caltech LIGO team who considered me capable enough and provided me with such a wonderful opportunity to explore the ever mysterious world of experimental physics.

The whole team at LIGO deserves a huge acknowledgement, but due the lack of space I will mention a few notable persons who deeply influenced throughout the course of the project. My mentor Dr. Eric Gustafson being first of them, for taking time out of his extremely busy schedule to listen to me and my ideas. Next, Zach who was a wonderful mentor, who taught me a great deal of everything from aligning cavities, to troubleshooting circuits. He was a real inspiration to me. I would like to specially thank him for taking time off his thesis project so that he could come work with me for hours at end. I would also thank my second mentor Dr. Rana for guiding me through some difficult portions of my project, for pointing out many of my mistakes and teaching me some very important lessons, his lessons have influenced me immensely. Finally a few other people who made my experience extremely pleasent are- Dr.Gabriele for being extremely affable and helping me out whenever I was stuck, Dr. Kate for helping me out occasionally in the lab.

I also must take this chance to thank all the LIGO SURF staff, Dr.Alan, especially for making this such a wonderful summer. The LIGO SURF administration staff which made all the bureaucracy look so easy.

Finally last, but not the least Dr.Kasivishvanathan and Dr. C.V.Krishnamurthy in IIT Madras for encouraging me to apply for this wonderful internship.

1 Introduction

Advanced LIGO(aLIGO)in its quest to detect Gravitational waves employs a Dual Recycled Michelson interferometer to read the relative phase difference in its two arms induced by a gravitational wave passing through it. These phase measurements like every other optical experiment, ultimately boil down to a current measurement with a photodiode.
The precision with which LIGO hopes to detect these waves places stringent requirements on the stability of the light power entering the interferometer. Undesirable fluctuations could originate from thermal drifts, mechanical resonances causing the laser resonator to change its length,polarization fluctuations etc. These are suppressed using various stages of passive noise suppression techniques, like triangular Fabry Perot cavity mode cleaners. Laser noise is further suppressed using active feedback techniques using photodiodes. The schematic for power stabilization employed in aLIGO is shown below in Figure-1. A detailed account of all such requirements can be found here[32].

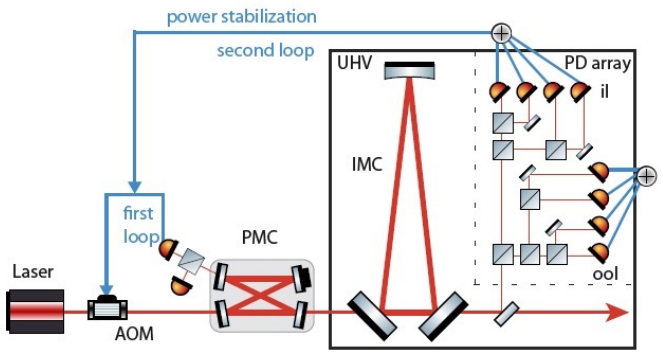

Figure 1: aLigo Power Stabilization Schematic

The passive part of this stabilization is to suppress spatial fluctuations(which could lead to beam jitter). Where as the power(intensity) fluctuations are suppressed using active feedback using photodiodes are various locations,placed both in in-loop configuration and out-of-loop configurations.

But the very process of measurement and hence final readout will be corrupted by various technical noises that plague the photodetector. It is this noise that is of concern for this project, especially noises which originate from nonlinear effects.

2 Motivation

This project wishes to investigate the excess noise that may accompany high photocurrent measurements in a photodiode. Unlike the Poisson shot noise which has a constant power spectrum, such a noise has a considerable portion of its power at lower frequencies and also depends on the current its being driven at. One could, in principle avoid this problem by reducing the light power falling on the photodiode by employing an array of photdiodes

each one detecting a small portion of the incident power. But the drawback that such a scheme faces is that such arrays are difficult to align and could lead to undesirable effects arising from spatial inhomogeneity of detectors or the complications accompanying the beam splitting arrangement, and hence desired accuracy is not obtained. Hence, if one could detect high photocurrent($\sim 200mA$) on a single photodetector, then one could do away with many of these complications, but this itself strings along with it excess current dependent noise. A group in France have reported very low noise levels in various photodiodes even at very high currents($\sim 182mA$)[1].The noise levels they have observed are as low as $2.4 \times 10^{-9} Hz^{-1}$. These results are promising, as now measurements would only be limited by the thermal noise in the detector.But the results seem to vary with the type of photodiode system and the measurement system used. Hence the motivation of this project is to study such excess current dependent noises in various varieties of photodiodes and investigate its properties.

3 Resistor Noise Modeling

In this section, We describe two possible models we investigated. The first model, models the noise as a noisy current source and the second one as macroscopic resistance fluctuations in the DUT(Device Under Test). The success/failure of the models illuminate the kind of processes that could cause such excess noise phenomenon.

3.1 Model 1-Current dependent noise in resistors

Excessive current noise can be traced to bunching and releasing of electrons associated with current flow, e.g. due to fluctuating conductivity based on imperfect contacts within resistive material[2].

A balanced Wheatstone resistor bridge setup will be excited with a low-noise constant power supply along one of the diagonal and the differential voltage between the other diagonal of the bridge will be analyzed after amplifying it with a low noise differential amplifier. The schematic for the experiment can be seen below in Figure 2

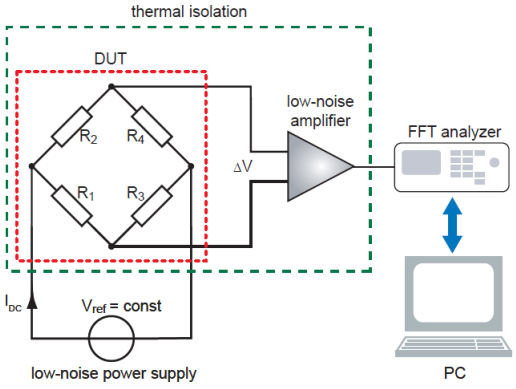

Figure 2: Schematic for the circuit for measurement of current dependent noise in resistors

The following presents a brief calculation: Let nominal values of the resistors be R_0 and the fluctuations in them be $\delta R_1, \delta R_2, \delta R_3, \delta R_4$.
Current in the circuit would then be $\frac{V_{ref}}{2R_0}$ through each of the two branches.

Calculating potential difference between the two ends of the other diagonal, one can verify that-

$$\Delta V = \frac{(\delta R_4 - \delta R_3)}{R_0} V_{ref} + \frac{i_4 - i_3 + i_1 - i_2}{2} R_0 \tag{1}$$

Where ΔV represents the voltage difference between the two diagonal nodes and i_3, i_4 represents the current noise in the corresponding resistors[1]. The first term is the common mode component, and second, the actual current noise present(this includes both the Nyquist-Johnson Noise and the additional excess current dependent noise we wish to measure). We would ideally want no contribution to the final output from the common mode, and hence we handpick resistors to match as close to each other as possible. A detailed result of such an experiment performed with various varieties of resistors can be found here [2]. We will be taking it a step further by analyzing this using the heterodyne demodulation scheme.

One could perform this experiment with a DC excitation but such measurements would require additional effort to isolate the resistor bridge from the surroundings to prevent undesirable effects arising from thermal drifts etc . Hence to avoid this we excite the setup with AC, which will modulate the noise, we then demodulate the output and analyze the resultant output. Such a modulation scheme lets us shift our noise to a frequency where our electronics components have much lower noise, and thereby increasing the SNR(Signal-to-Noise Ratio).
This experiment will also serve as good place to be introduced to the data analysis techniques employed in such noise measurements and which will be used in the second half of this project with photodiode noise.

3.1.1 Modeling of the excess noise

The model developed is based on the work done on excess current noise in resistors with applied DC voltage. It was conclusively proved that the magnitude of noise is a linear function of the applied DC drive and that the amplitude spectrum is a $\frac{1}{\sqrt{f}}$.Which can be seen in Figure 3 and Figure 4, taken from [2].

We wish to develop a experimental method to characterize this excess noise spectrum and calculate its power in the bandwidth of interest. The following presents the detailed mathematical calculation and associated assumptions.

Let i_e be the excess current noise. We model the excess current noise as following:

$$i_e(t) = \alpha f(V_{drive}) g(t) + \beta \tag{2}$$

[1]This can be easily verified by applying Kirchoff's current law at the nodes of interest

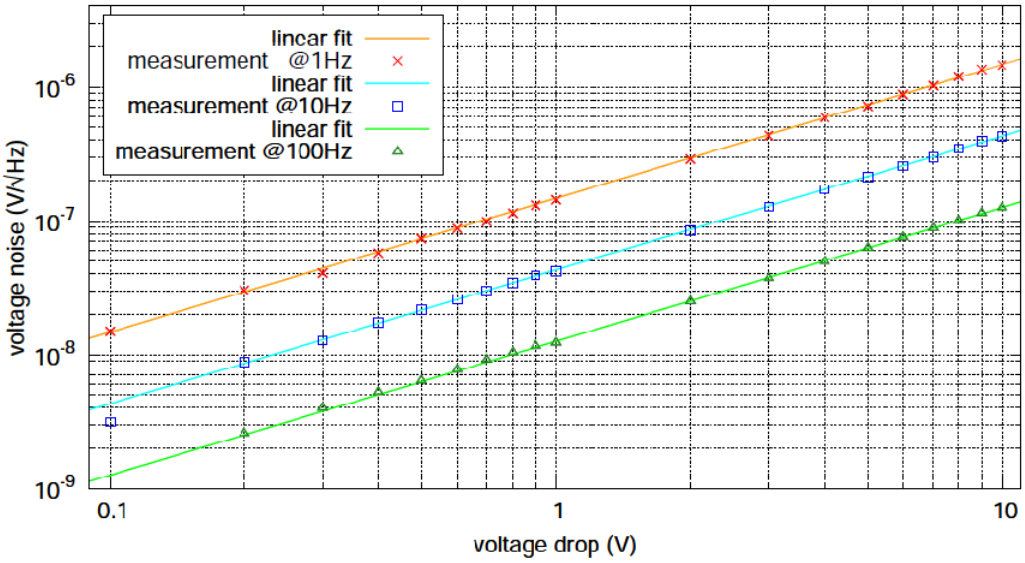

Figure 3: Noise Magnitudes at 1Hz,10Hz and 100Hz as a function of Drive Voltage. The noise amplitude is linear with applied drive voltage

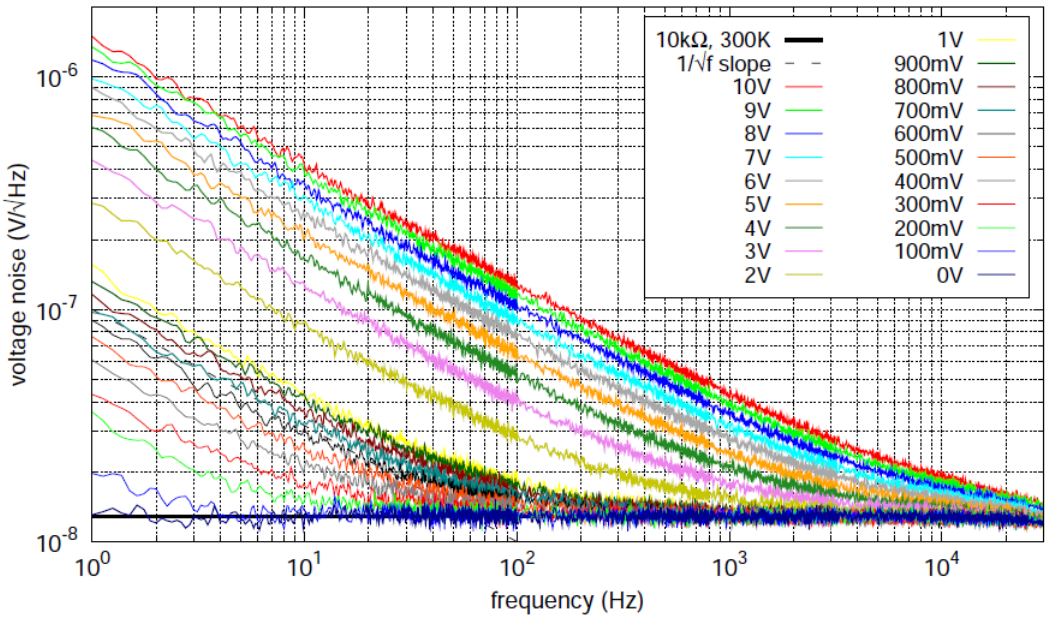

Figure 4: Spectrum of excess noise in resistors as measured at DC as a function of drive voltage

Where alpha is, typically, this would depend on the method adopted for manufacturing the resistor(eg:Thick Film Resistor, Thin Film, Wire Wound etc).$f(V)$ is some function through which the excess noise depends on the drive. DC voltage measurements confirm that the resultant noise is linear, so, we can assume f(V_{drive}) to be a linear function of V_{drive}. Also, at $V_{drive} = 0$ the excess noise is absent, this suggests that β in the model must be zero. $g(t)$ is the underlying stochastic process which governs this noise. DC measurements have confirmed that this stochastic process is a $\frac{1}{f}$ process. This finally reduces to:
$i_e(t) = \alpha f(V_{drive})g(t)$
We now estimate the form of $f(V)$, since the two nodes at which drive is applied are completely equivalent, suggests that i_e cannot change signs with drive. Hence it must have the $|h(V)|$, where $h(V)$ is some function, this intrinsically contains the symmetry as mentioned above. DC measurements have established that the noise has a linear dependence on the input drive hence we start by saying $f(V_{drive}) = |V_{drive}(t)|$, ie the excess noise depends on the absolute value of drive. This model is compatible with all the previous results obtained at DC and will be the starting point for our AC analysis.
Let, the drive be a pure sinusoidal one. i.e $V_{drive}(t) = V_{0d}\sin(\omega_0 t)$, where V_{0d} is the peak amplitude of the drive and ω_0 is the input drive's angular frequency. Then according to the our model:

$$i_e(t) = \alpha|V_{0d}\sin(\omega_0 t)|g(t) \tag{3}$$

The $\sin(\omega_0 t)$ can be expanded as a sum of its Fourier coefficients as follows:

$$|\sin(\omega_0 t)| = \frac{2}{\pi} - \frac{4}{\pi}\sum_{n=even}\frac{\cos n\omega_0 t}{n^2-1} \tag{4}$$

It can be seen that this has a large DC value of $\frac{2}{\pi}$ and only even harmonics and their contribution decreases as $\sim n^{-2}$ hence higher harmonics have very less contribution. Owing to this we terminate this series at the second harmonic:

$$i_e(t) = \alpha(a_0 + a_2\cos(2\omega_0 t)g(t) \tag{5}$$

Where a_0 and a_2 refer to the Fourier series coefficients $\frac{2}{\pi}$ and $\frac{4}{3\pi}$ respectively.

3.1.2 Simulations

Quoting equation 1

$$\Delta V = \frac{(\delta R_4 - \delta R_3)}{R_0}V_{ref} + \frac{i_4 - i_3 + i_1 - i_2}{2}R_0 \tag{6}$$

This can be separated out into two components- one of which is because, the resistors have not been matched perfectly and second is the excess noise we wish to measure.

$$\Delta V = V_{mis}(t) + V_{noise}(t) \tag{7}$$

Where V_{mis} is the mismatch voltage that occurs because of the mismatch between resistors and V_{noise} is voltage as a result of noise processes(like excess noise, thermal noise etc). V_{noise} as previously stated can be written as:

$$V_{noise} = \frac{i_{tot4} - i_{tot3} + i_{tot1} - i_{tot2}}{2} R_0 \tag{8}$$

Where i_{tot} refers to the sum of excess current noise and thermal noise. This is a incoherent addition of 4 identical and uncorrelated random processes. The total power spectrum of this differential voltage would then just be the same as that for a single resistor. Therefore:

$$\begin{aligned} V_{noise} &= i_{tot} R_0 \\ &= (i_e + i_{th}) R_0 \\ &= (\alpha \left|V_{drive}(t)\right| g(t) + i_{th}) R_0 \\ &= (\alpha \left|\sin(\omega_0 t)\right| g(t) + i_{th}) R_0 \\ &= (\alpha(a_0 + a_2 \cos(2\omega_0 t) g(t) + i_{th}) R_0 \end{aligned} \tag{9}$$

This procedure was simulated on MATLAB. The underlying stationary process was assumed to be $\frac{1}{f}$ spectrum. First, a time series for the $\frac{1}{f}$ was simulated using an code found at[3]. Shown in Figure 5 and Figure **??** are the simulated time series and its spectrum

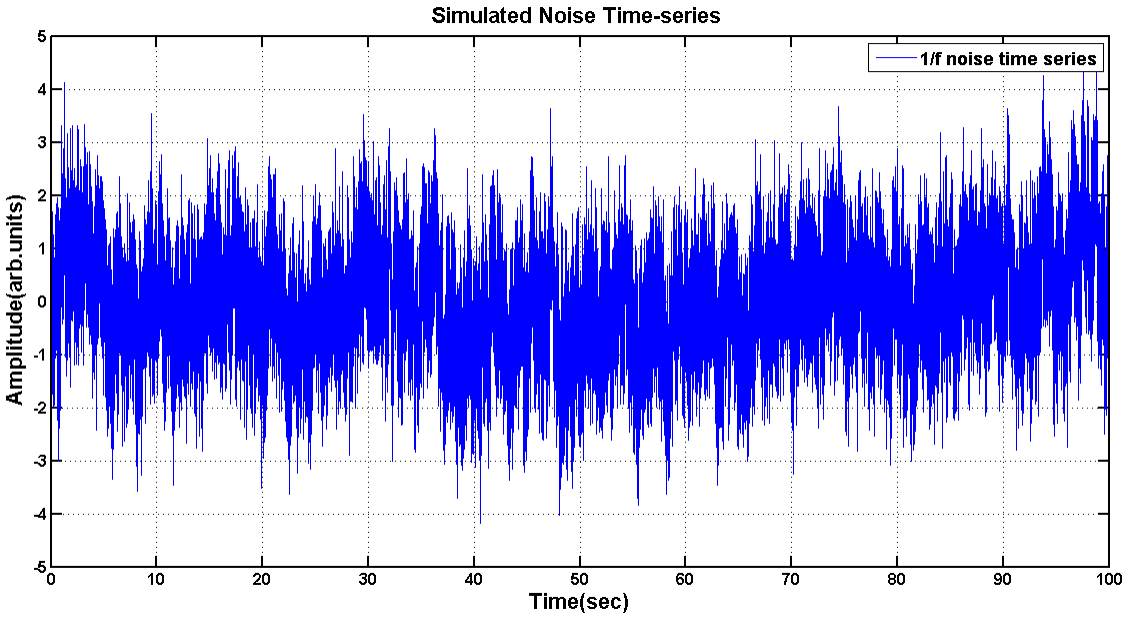

Figure 5: $\frac{1}{f}$ timeseries

This time series, according to our hypothesis will be amplitude modulated(multiplied) with a absolute sine wave to simulate the noise that we expect to see as the differential bridge output. Figure 7 is the drive modulated power spectrum of the noise.

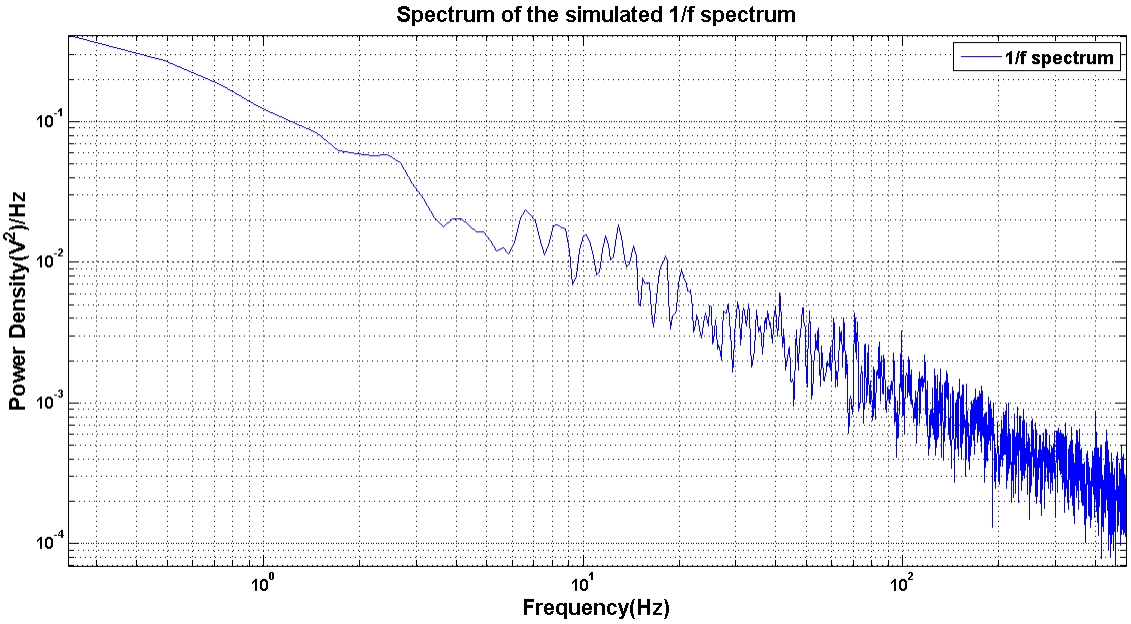

Figure 6: Spectrum of the above simulated time-series, it can be clearly seen that has a $\frac{1}{f}$ power spectrum

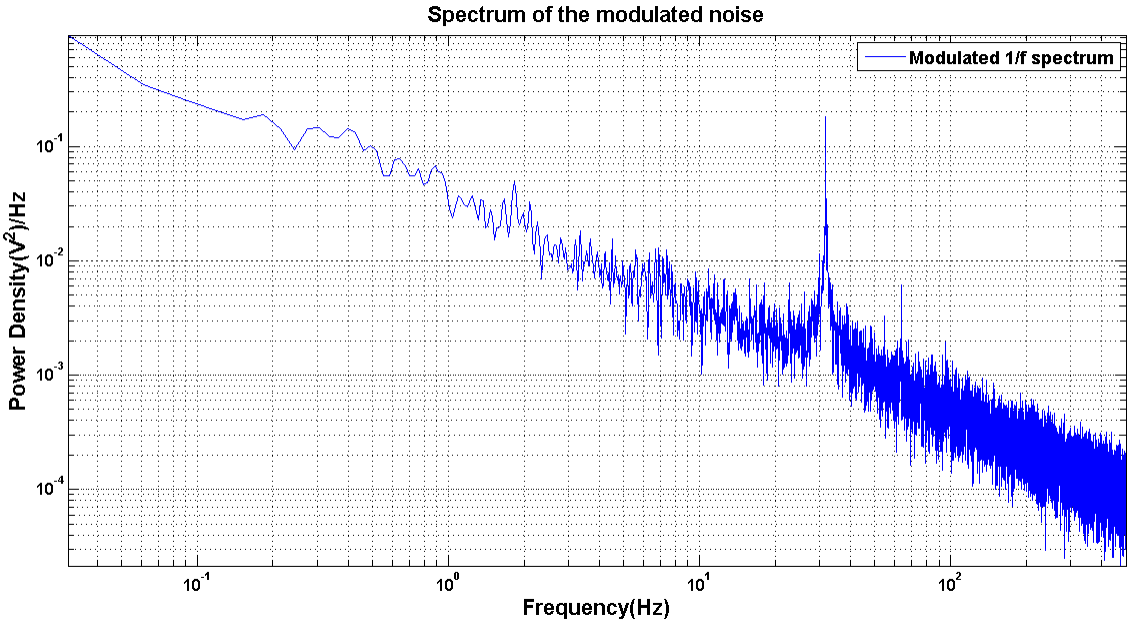

Figure 7: Spectrum of the modulated noise

Notice the peaks at $2\omega_0$, $4\omega_0$. As predicted a considerable power remains at lower frequencies because the fourier series expansion of $|\sin \omega_0 t|$ has a coefficient at DC. This signal is demodulated at $2\omega_0$ and then passed through a low-pass filter. This is done by a lock-in amplifier. The lock-in uses the input drive as a reference and then generates a reference at twice the frequency which is used to demodulate the amplifier's output. The demodulated power spectrum is shown in Figure 8.

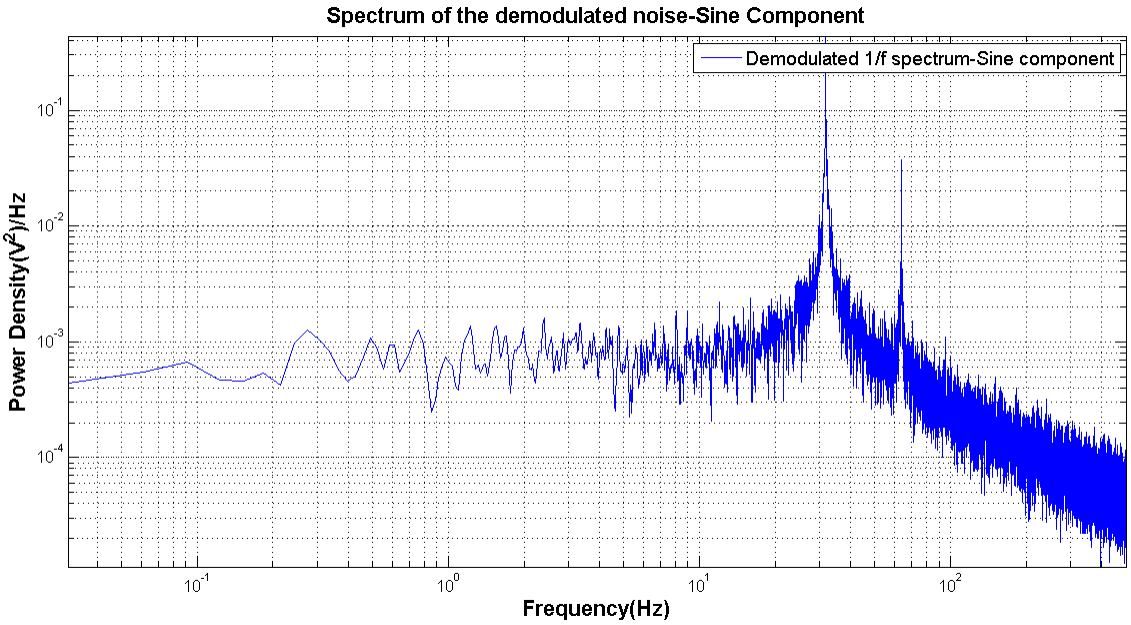

Figure 8: Power spectrum of the modulated noise

The component at $2\omega_0$ as shifted to DC because of the demodulation. We can low pass this resultant filter to isolate the demodulated signal's spectrum at DC. Provided that such a model is correct this method of detection should be able to isolate the spectrum of underlying stochastic processes governing this excess noise. The conditions in the simulations above were perfect with no external limiting sources like thermal noise, Amplifier noise etc. These will be considered in the subsequent sections.

3.1.3 Experimental Schematic

Figure 9 describes the experimental schematic proposed for such a measurement: The

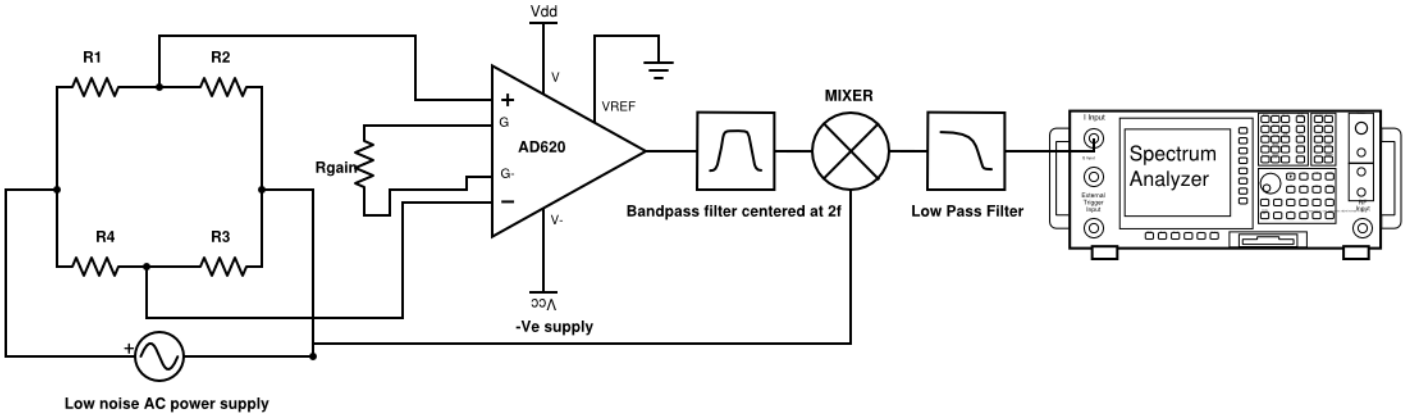

Figure 9: Schematic for measuring excess noise in resistors

schematic is easy to comprehend. The voltage difference as mentioned in equations 1 is sensed between the two diagonal nodes of the wheatstone bridge. This node will have a component at the frequency of the drive applied, this corresponds to the mismatch component and we expect to see the noise side-bands at $2\omega_0$. This is amplified using a low noise instrumentation amplifier(AD620). This amplifier has high common mode reduction ratio(CMRR) and a very low noise floor of $9nV/\sqrt{Hz}$ at 1kHz. The gain is adjustable by adjusting the gain reisistor, we used a 100Ω resistor to obtain a gain of 500. The drive frequency selected by us was $1kHz$.This frequency was chosen keeping in mind the bandwidth of the amplifier which is for a gain of 500 would be $24kHz$. This signal is passed through a bandpass filter which was realised using a SR650- Dual channel programmable filter. The filter bandwidth used was $200Hz$ around $2\omega_0$. This is fed as an input to a lock-in amplifier-SR830, the drive frequency is fed as the reference input to it and the second harmonic generated within the lock-in is used to demodulate the band passed output. This is then finally input to the low pass filter and its time constant was set at $\sim 1ms$.

3.1.4 Experimental Results

The following are the experimental results by applying the above mentioned model:

1. The direct spectrum of the differential bridge voltage power spectrum can be seen in Figure 8. The large peak corresponds to mismatch component which at the drive frequency which was $1kHz$ and we expect to see the excess noise around $2\omega_0$ which is $2kHz$.

2. The band-passed output at $2\omega_0$ can be seen in Figure 9, the bandwidth of the band pass was $200Hz$ on either side of $2\omega_0$.

3. Figure 10 demodulated output. Lock-in amplifier's low pass filter was set at 30Hz with a roll off of -24dB/oct.

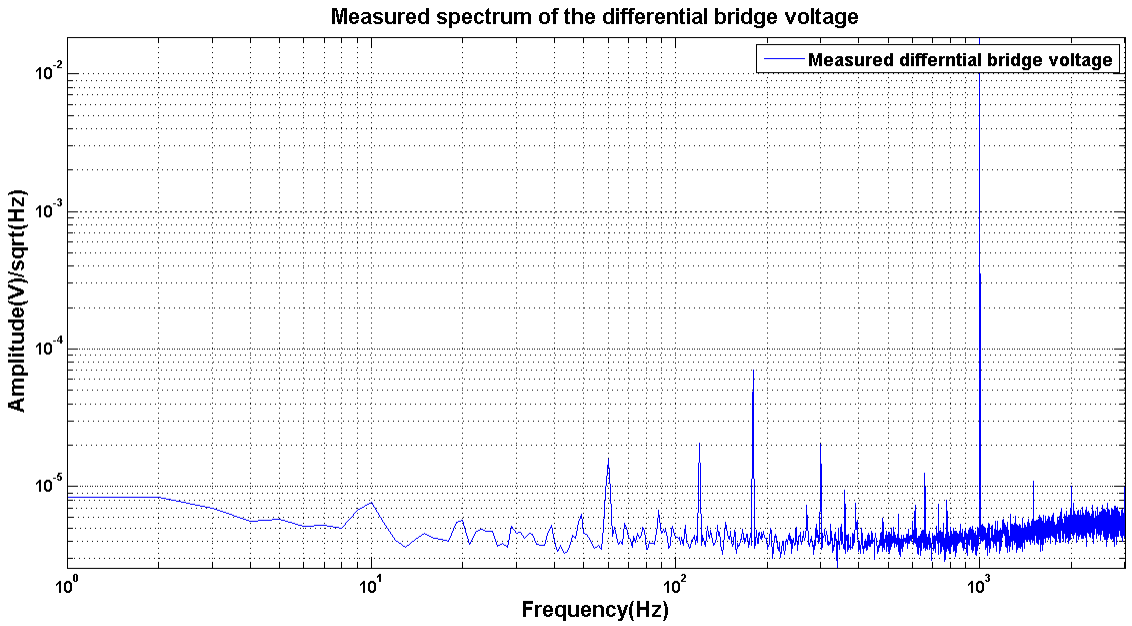

Figure 10: Amplitude spectrum of the differential bridge output

So far no observation of $\frac{1}{f}$ noise could be done by this scheme, this could imply two things- one, that some part of the experiment is limiting the measurement of this by raising the noise floor thereby preventing us from detecting it or second, the model itself is flawed and that the idea of looking at the $2\omega_0$ frequency is incorrect.

3.1.5 Drawbacks associated

One of the limitations with such a scheme is that it is limited by the thermal noise background, i.e. excess noise below thermal noise cannot be measured with this technique. The part of spectrum that is above the noise floor can be measured, as a lock-in cannot selectively distinguish between two broadband noise sources. Such a scheme will be limited by the background noise.

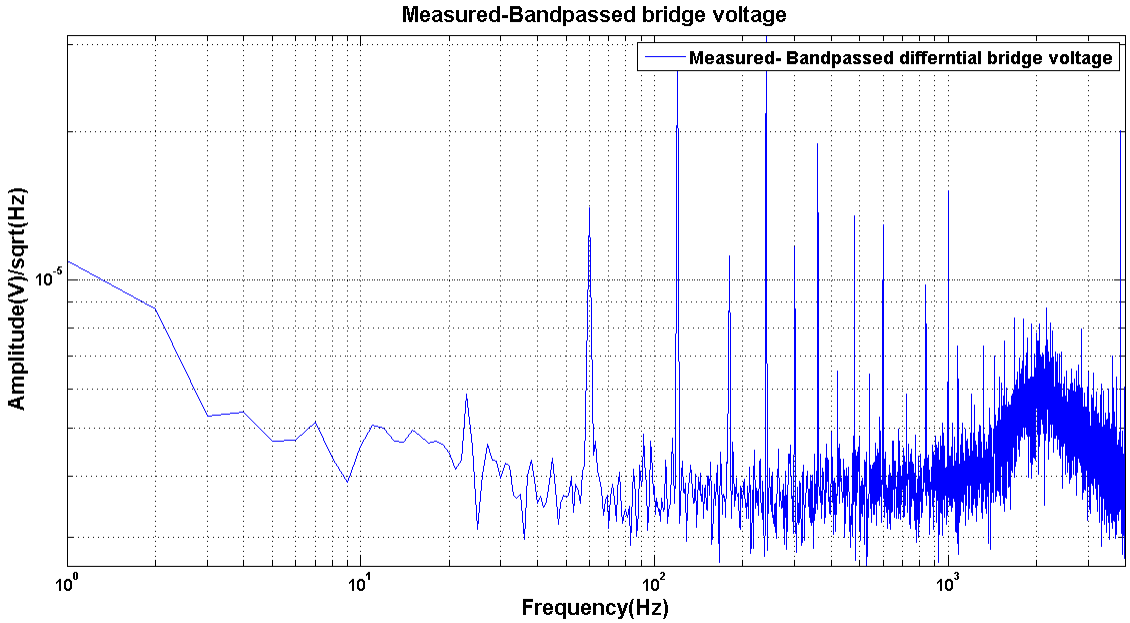

Figure 11: Spectrum of band-passed bridge voltage, notice how the all the other frequencies have been attenuated

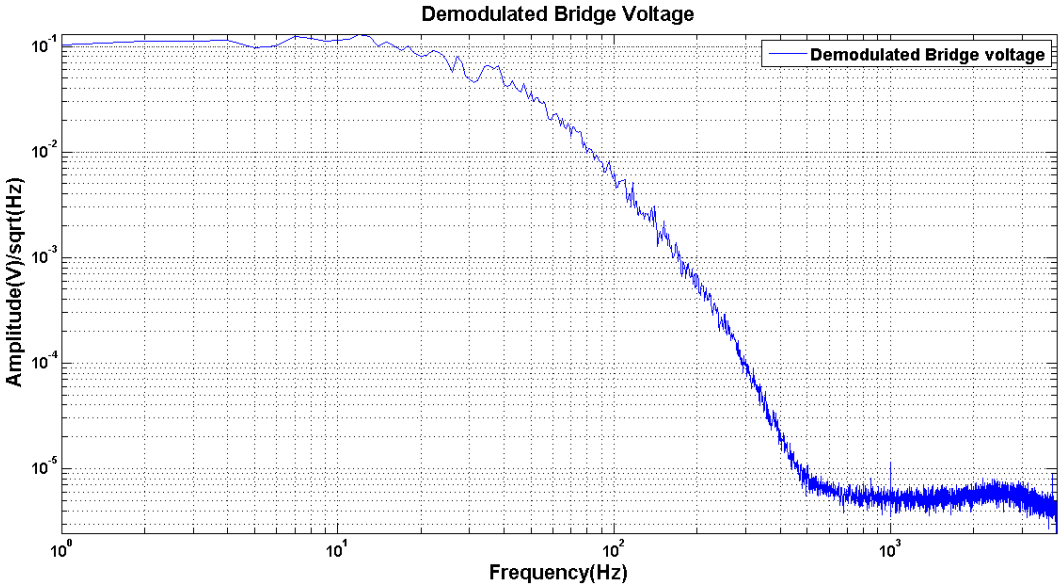

Figure 12: Amplitude Spectrum of the in-phase component of demodulated output

3.2 Model-2: Resistance fluctuations

3.2.1 Reasons for the failure of Model-1

In the Previous section resistor's voltage fluctuation was modeled via a noisy current source:

$$i_e(t) = \alpha |V_{drive}| g(t) \tag{10}$$

As before, $i_e(t)$ refers to the excess current noise,α refers to some constant which depends on the resistor type and $g(t)$ refers to an underlying stochastic process. The voltage dependent function was modeled as : $|V_{drive}|$. It is worthwhile to analyze what such a model means. The above hypothesis assumed that the noise was produced by "current sources" inside the resistor which manifested as voltage noise when voltage was measured across the bridge. In this model, modeling the voltage dependence with a 'absolute sign' makes sense, because the direction in which the noise sources inject current is independent of the direction of drive current. But, resistors are passive devices and modeling a current source as reason for excess noise is not intuitive, it is more natural to model the noise as a manifestation of fluctuating resistance, i.e the electrons inside the resistor could be subject to various kinds of material defects, which microscopically appear as a fluctuating conductance or resistance. The bias current is just a way to probe these fluctuations. The resultant voltage fluctuations will then be dependent on the direction of the bias current. With this as an inspiration, a second model is described in following sections.

3.2.2 Modeling the fluctuations

As stated above, the fluctuations now are modeled as resistance fluctuations and not current fluctuations. The circuit to be analyzed would then look like Figure:13, where each test resistor has been assigned with a random resistance fluctuation(δR_1 , δR_2, δR_3, δR_4).

It is then straight forward to prove that the resultant voltage as measured across the bridge would be(see Appendix A)-

$$\Delta V = \frac{(\delta R_2 + \delta R_3 - \delta R_1 - \delta R_4)}{2R_0} V_d \tag{11}$$

Where ΔV refers to the differential bridge voltage, R_0 refers to the nominal resistance of each of the resistors, and V_d is the drive voltage. Previous studies done on resistors for DC bias voltages have shown that the excess voltage noise is linear function of drive voltage(see [8],[2]). This would imply that δR's would have to be stationary random processes, as the differential voltage already has a drive dependence(V_d outside the fraction). This is in accordance with one's intuition, because this model assumes the source of such fluctuations to be due to material defects (these must be independent of everything else like drive voltage etc) and hence they must be stationary.
Let the net resistance fluctuation(ie incoherent sum of the four uncorrelated resistance fluctuations) be denoted by $\delta R(t)$. The differential bridge voltage now reduces to :

$$\Delta V = \frac{\delta R}{2R_0} V_d + V_m \tag{12}$$

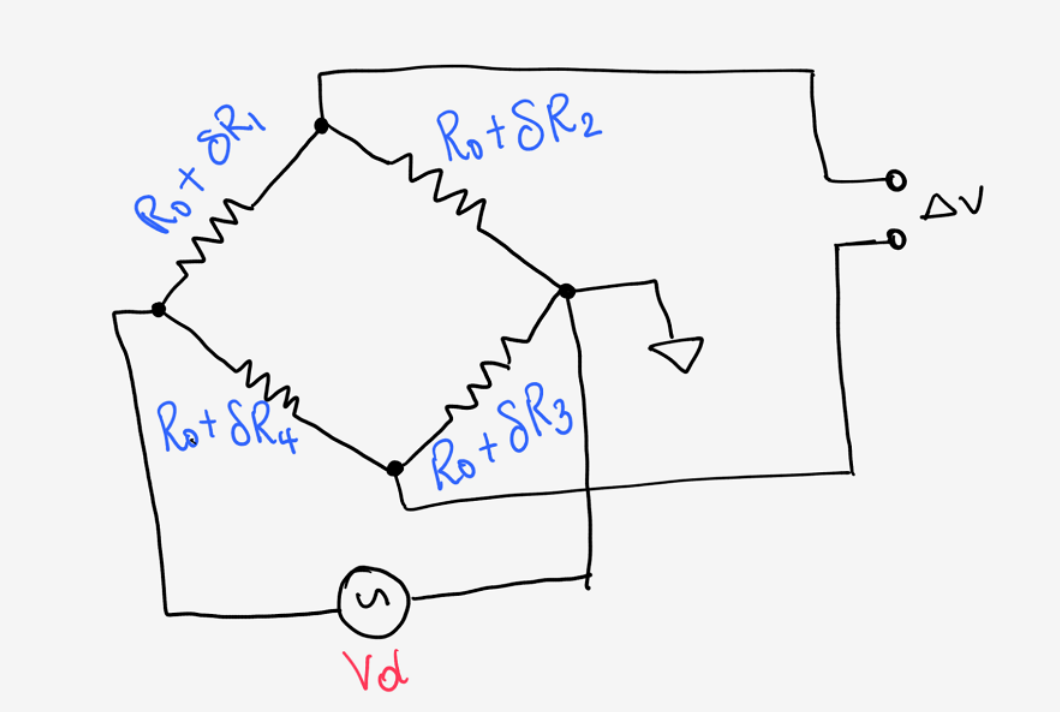

Figure 13: Schematic for the circuit for measurement of current dependent noise in resistors

Here, V_m refers to the differential bridge voltage due to residual mismatch between the resistors in the bridge.

Let the drive voltage applied be a sinusoidal $V_d = V_0 \sin \omega_0 t$. It can be formally proved that the resultant power spectrum of the differential bridge voltage would be(it would be easy to assume that since the auto correlation of such a process would be time dependent one cannot define a power spectrum for it)[2]

$$S_{\Delta V}(\omega) = S_m(\omega) + i_0^2 \frac{S_{\delta R}(\omega - \omega_0) + S_{\delta R}(\omega + \omega_0)}{2} \tag{13}$$

$S_{\Delta V}(\omega)$,$S_{\delta R}(\omega)$,$S_m(\omega)$ refer to the power spectra of bridge voltage, resistance fluctuation and mismatch component respectively. i_0 refers to the current through the each of the resistors which is $\frac{V_0}{2R_0}$. The differential voltage arising due to imperfect matching of resistors would just appear as a Dirac delta function(as it would be a pure sine wave) in the total power spectra, since we are interested in the spectrum around ω_0 it could very well be left out when

[2]such processes where a random stationary process is amplitude modulated by a periodic signal are called cyclostationary processes and its a subject in its own right. For some good resources on this subject see : [24], [25], [26]

carrying out analysis.
This differential bridge voltage is band-passed around ω_0 and demodulated and low passed using a lock-in amplifier. It can be algebraically be proved(see Appendix B, [8], [10]) that resultant power spectra at the output of the lock-in would be:

$$S_{net}(\omega) \simeq G_0^2 \left[S_V^0(\omega_0 - \omega) + i_0^2 S_{\delta R}(\omega) \cos^2\theta \right] \tag{14}$$

Where S_V^0 is the power spectra when zero drive is applied(that is, it would refer to the background noise),G_0 is the combined gain of the lock-in amplifier, instrumentation amplifier, bandpass filter and the low pass filter, θ refers to the phase difference between the input and the lock-in's internal reference. The advantage of such a method is its phase sensitivity. At $\theta = 0°$ the output power spectra is the sum of power spectra of resistance fluctuations and background noise, where as at $\theta = 90°$ the output spectrum is just the total background noise! It isolates the background noise spectrum and allows for a measurement of just the excess noise. But that being said, one should not get the notion that one can do measurements to arbitrary precision below the background noise level. Though there are methods which allow for measurement below the background noise spectrum, these are described in a later section. This method is called the $'0 - 90$ subtraction method and it can be used to probe any kind of excess noise spectrum(see [8], [10]) for a detailed description of this method). This method has been extensively to study excess noise spectra in solids([10]), semiconductors([23]), tunnel junctions([22]). Such excess noise processes give a lot of information about relaxation processes in solids especially useful in condensed matter physics(also see[5], [6] for some beautiful written descriptions of excess noise processes).

3.2.3 Experimental schematic

The experimental schematic is shown in Figure-14, and the actual circuit is shown in Figure-15. The setup consists of a resistor bridge, the resistors were hand matched to $\sim 0.05\%$. The setup was soldered on a circuit board to avoid error due to improper contacts. The differential bridge voltage is then amplified by a instrumentation amplifier AD620, which has a low noise level($9nV/\sqrt{Hz}$ at $1kHz$) and can be programmed for any desired gain with one resistor. For this application, a 499Ω resistor was used which corresponds to a gain of 100. Output of the amplifier is connected to a bandpass filter, we used a cascaded high pass-low pass filter using a SRS650- dual channel programmable filter. The output of the band-pass filter was then fed into a SR830-DSP lock-in amplifier. This lock-in is especially useful because of its dual output consisting of both in-phase and quadrature components, very low phase error and very high harmonic rejection(see [27], [28]). The two outputs of the lock-in were recorded using a DAQ which has a sampling rate of 16384 samples/sec.

3.2.4 Results

In this section, we present our experimental results. Figure-16 shows the power spectrum of the Differential bridge bridge voltage. This spectrum is for a $1.5k\Omega$ Carbon-Film(CF) reisistor driven at $1kHz$ with a peak amplitude of 5V. The large peak is due to the fact that resistors are not perfectly matched(the mismatch component), the excess noise is expected

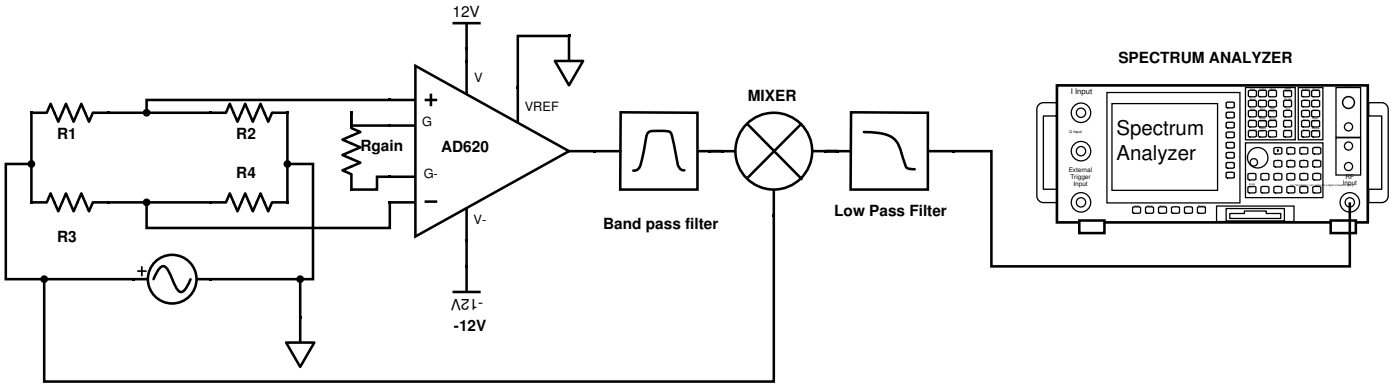

Figure 14: Schematic for the circuit for measurement of current dependent noise in resistors

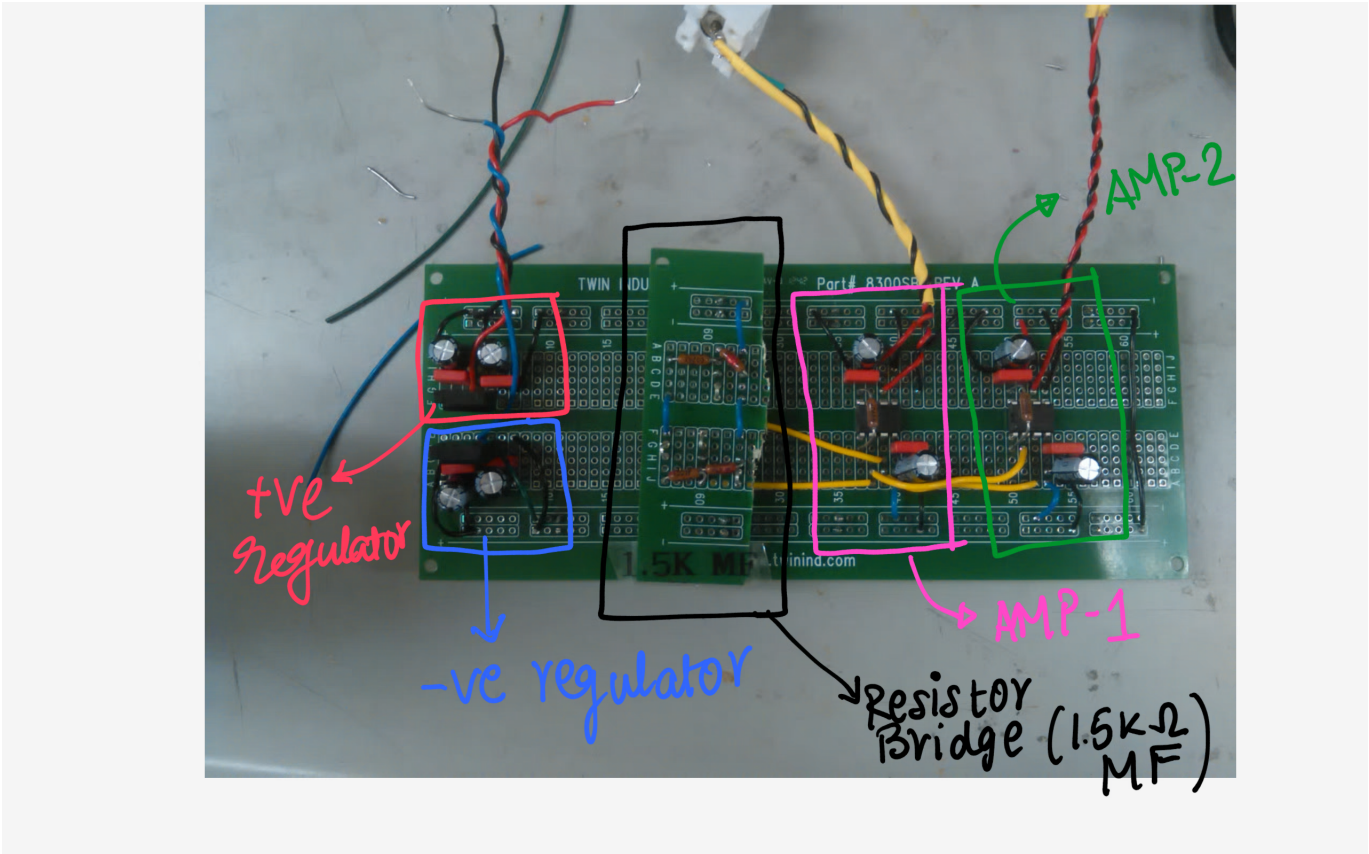

Figure 15: The constructed circuit

to be around within a range of $\sim 100Hz$. The source was derived from the 'sine out' of SR830-Lock-in amplifier.

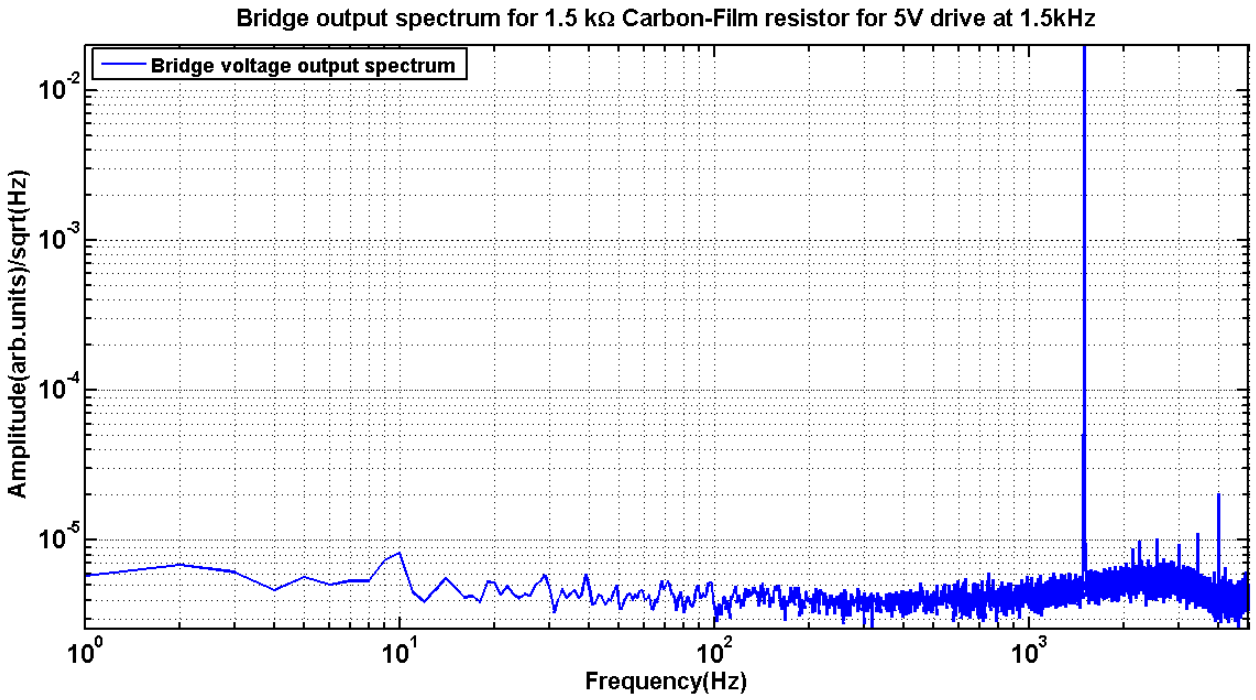

Figure 16: Amplitude spectrum of amplified bridge voltage

This is then band-passed using SRS650 and then locked in using SR830 the final output spectrum is shown Figure-17.
Since resistors also have finite capacitance, this leads to an additional phase mismatch which was not compensated for, which is why the background noise is not completely flat as one would expect, but has the same profile as the in-phase(the θ we defined in 14 is not exactly zero for the in-phase component). One could connect a variable capacitor across one of the resistors to compensate for this phase mismatch(see [4], [5])

3.2.5 Characterizing measured excess noise

In this section the excess noise obtained is characterized as a function of various parameters like resistor type, drive voltage, drive frequency. Figure-18 shows the excess noise spectrum obtained as a function of drive voltages for drive frequency of $500Hz$ for a drive voltage range of $0V - 1V$.
Similar plots were generated for drive frequencies of $1kHz$, and $1.5kHz$ which are shown in Figure 39, Figure 38 in Appendix- C.

Some inferences worth noting from these plots are:

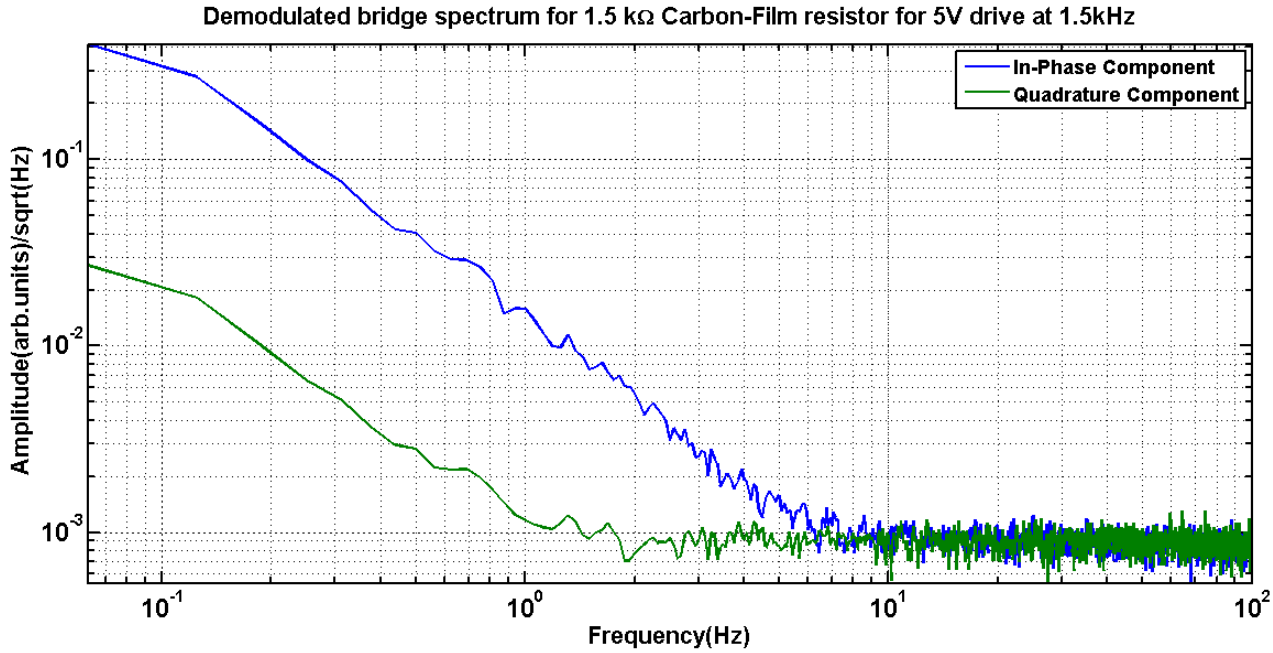

Figure 17: Output Spectrum- showing both in-phase and quadrature components

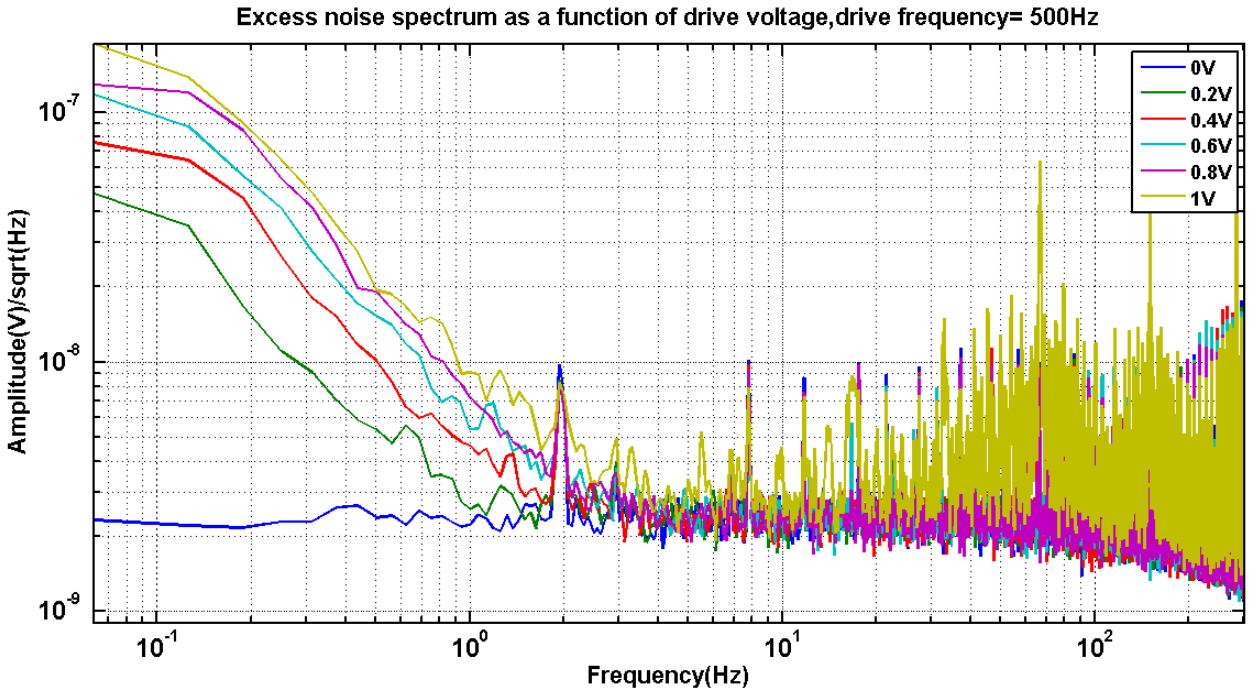

Figure 18: Excess noise spectrum as a function drive voltage(0V to 1V) for a drive frequency of 500Hz

- The background noise level is the same in all the plots.
- Excess noise has a strong dependence on the drive voltage but a weak dependence on frequency

The the roll off seen at around $100Hz$ is low pass response of lock-in's low pass filter, which was set at $100Hz$ with a roll off of $-24dB/decade$.

The exact dependence of the excess noise on drive voltage is found by plotting the excess noise magnitude at $1Hz$(or any frequency for that matter) as function of drive voltage. Figure 19 shows the amplitude of excess noise at $1Hz$ as a function of drive voltage, for a fixed drive frequency of $500Hz$. A roughly linear dependence of the excess noise is clearly visible as hypothesized in the model. The plot has a slope of 2.54×10^{-3} $arb.units/V\sqrt{Hz}$.

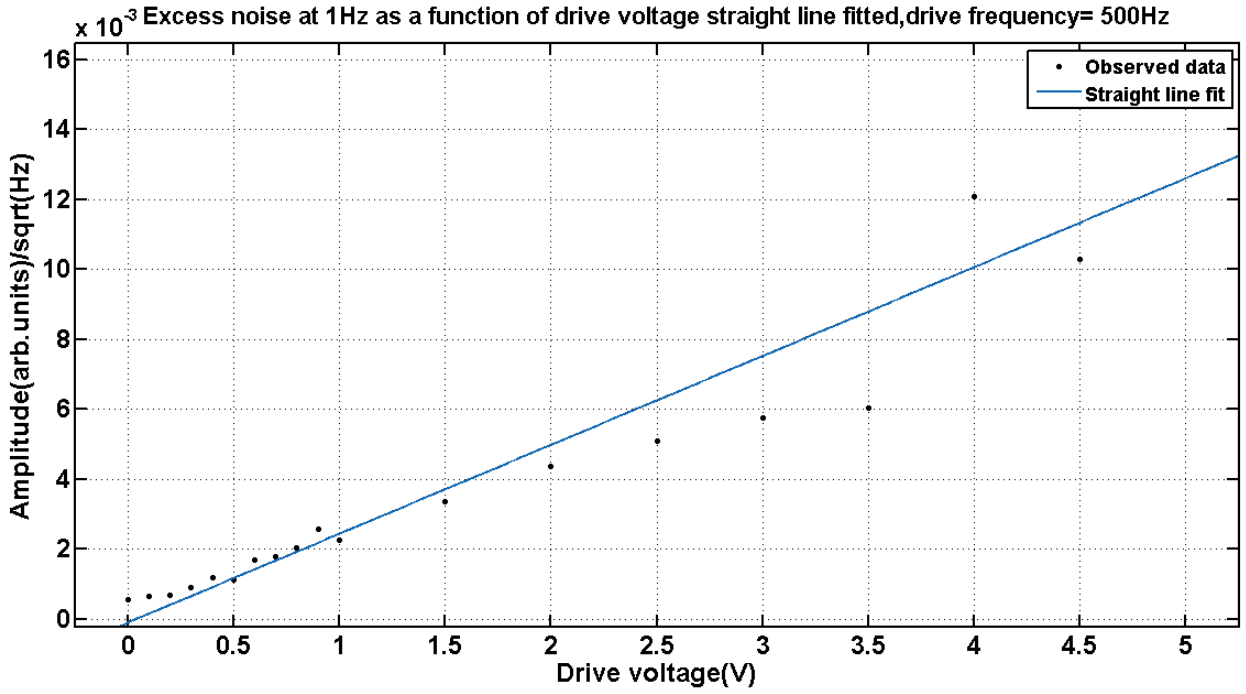

Figure 19: Excess noise spectrum at 1Hz as function of drive voltage- straight line fitted for a drive frequency of 500Hz

The frequency dependence of the in-phase component of this excess noise was studied for frequencies from $500Hz$ to $6.5kHz$ this upper limit was chosen because the DAQ used has a sampling rate of $16ksamples/sec$ and any frequency above $8kHz$ would be aliased. Figure 20 shows the in-phase component of the excess noise as a function of frequency. With the lock-in's phase has been kept constant at $0°$ the in-phase component starts decreasing with increasing frequency, because the phase mismatch due to capacitance of the resistor increases.

Another factor on which excess noise depends, is the resistor type. The material defects causing such fluctuations depend on the quality and the method using which the resistors

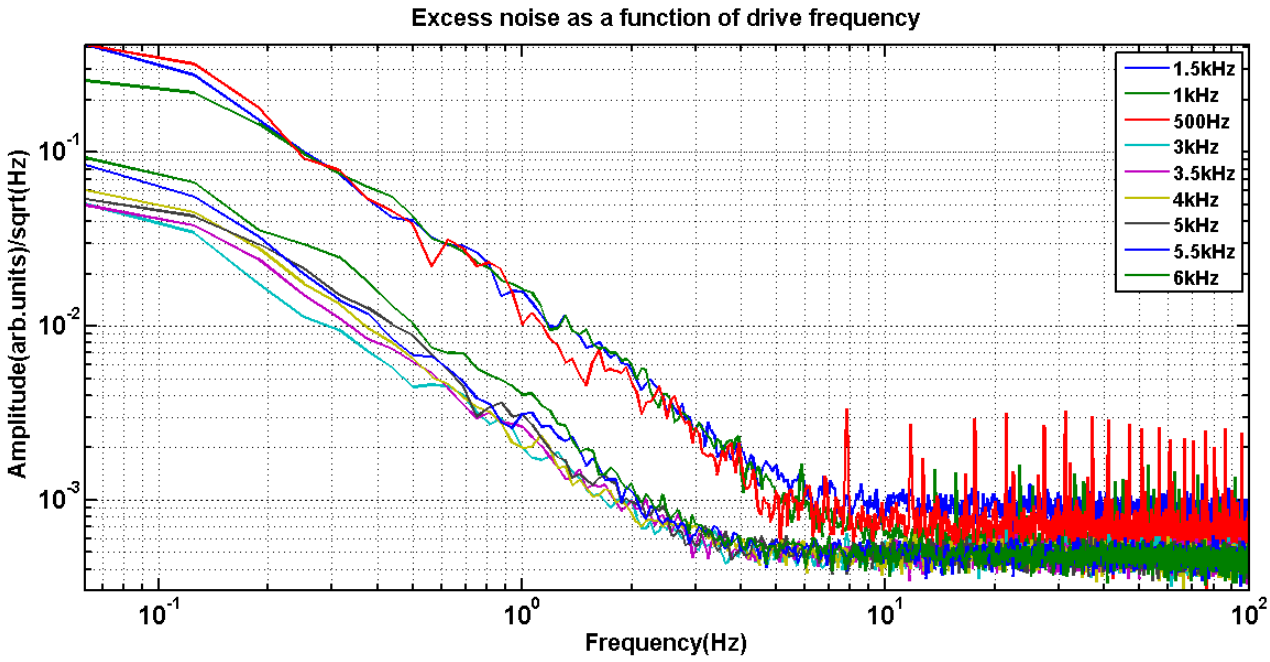

Figure 20: Excess noise spectrum as a function frequency for a drive voltage of 5V

were manufactured. This experimental setup was used to measure excess noise in Carbon-Film resistor(CF) and Metal Film resistors(MF). According to literature(see [8]) fluctuations in metal film have been reported to be 2 orders of magnitude smaller then those in carbon-film ones. Figure 41 in Appendix-C is the excess voltage noise observed in $1.5k\Omega$ MF resistor as a function of drive voltage[3].Points to note are:

- Linear behavior with drive voltage.
- Background noise is almost the same as that for $1.5k\Omega$ CF resistor
- Excess noise is 2 orders of magnitude less than CF resistor, in agreement with literature.

Another parameter worth studying is the dependence of excess noise on the resistor value. If the resistance of the sample is reduced then current in it would increase resulting in a larger voltage fluctuations. This was verified by measuring the excess voltage noise for a bridge consisting of 200Ω MF resistors. Additionally resistance fluctuations could depend on the dimensions of the resistor, but these have not been studied. Figure-40 in Appendix-C shows the excess voltage noise observed in 200Ω MF resistors and Figure-21 shows a comparison between $1.5k\Omega$ CF, $1.5k\Omega$ MF and 200Ω MF resistor[4].

Key points to note are:

[3]the cutoff of lock-in was set very small around $3Hz$ because line interference(for some reason) was very large. The cutoff was chosen such that it does not mask any important features

[4]Excess line-harmonics were also observed for 200Ω MF resistor, so a $3Hz$ low pass cutoff was kept for this sample as well

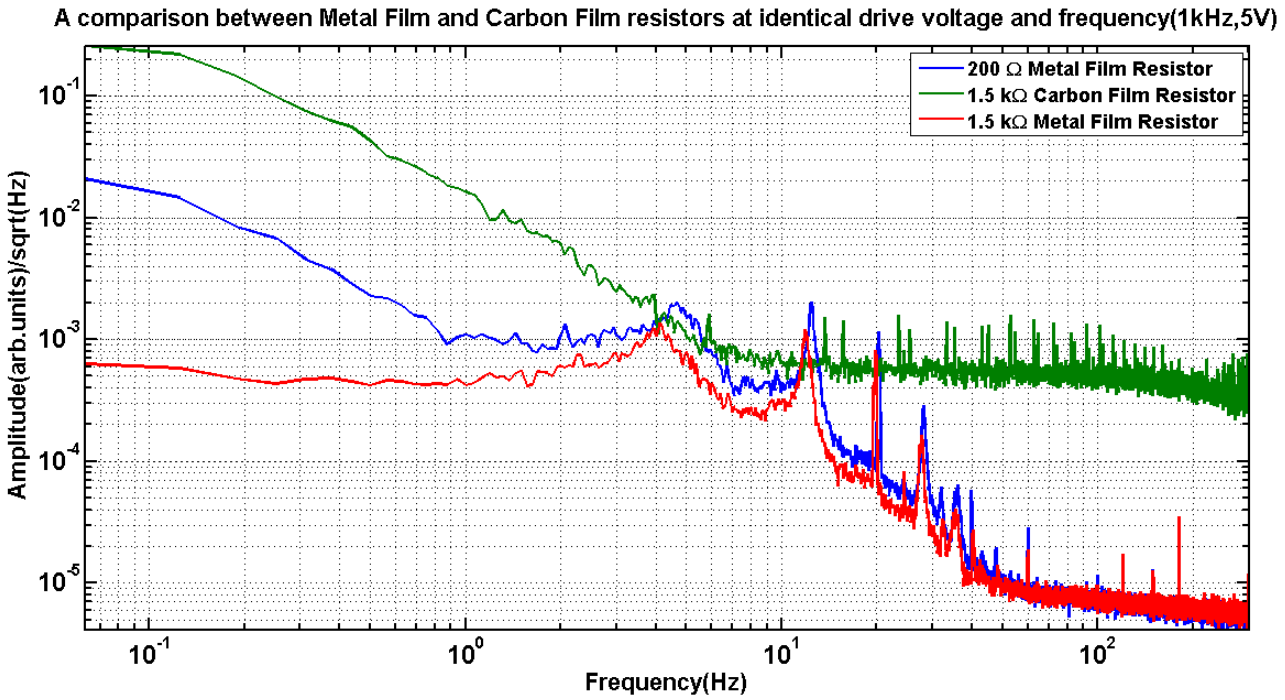

Figure 21: Comparison of excess noise in $1.5k\Omega$ CF,$1.5k\Omega$ MF and 200Ω MF resistors under identical drive conditions

- As expected the the excess voltage fluctuations in 200Ω MF are almost an order larger then $1.5k\Omega$ resistors.
- The background noise in all of the resistors is approximately the same. This is because the background noise is limited by the instrumentation amplifier's noise which is a order more than thermal noise of the resistors used(see Appendix D for noise plots of various instruments used).

Finally we characterize the the shape of the obtained spectrum, its evident that it is not a $\frac{1}{\sqrt{f}}$ spectrum but something more steeper than that, which is in disagreement with the literature[5]. Following is a straight line fit on the observed excess noise spectrum in its linear region(~ 0 to $10Hz$) for a $1.5k\Omega$ CF resistor for a drive voltage of $5V$. The observed spectrum had a slope of $-1.383(-1.412, -1.355)$ where the numbers in the brackets are the 95% confidence bounds on the slope. Figure-22 shows the straight line fit.

3.2.6 Possible reasons for the the observed inconsistency

The fact that the observed spectrum is almost twice as steep as what is expected, is something worth wondering as to why such a result was observed. Here, in this section we present a few possibilities :

[5]It is well established that resistance fluctuations have a spectrum of $f^{-0.5}$

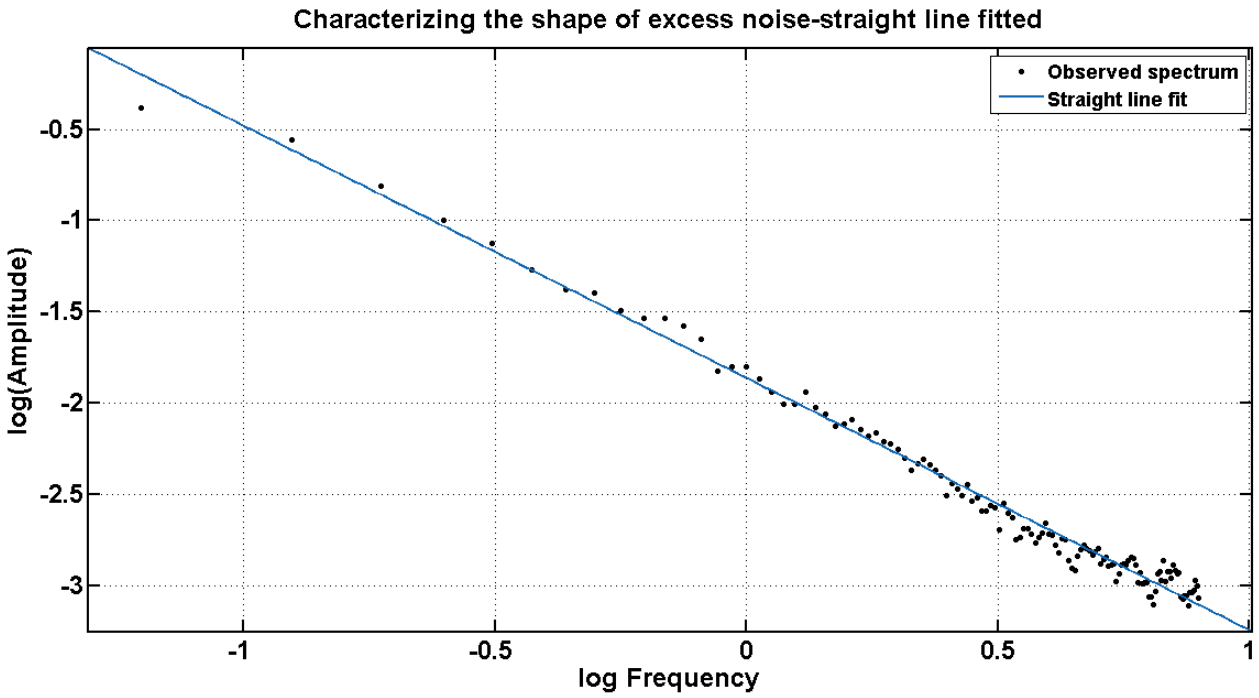

Figure 22: Characterizing the shape of obtained spectrum

- The most likely of the hypothesis is that, an error went unnoticed in our experimental schematic. Even though the experiment was constructed with extreme care, it is possible that the experimental setup had an error that we were unaware of.
- A trouble-shooting attempt was performed to isolate, the source producing these results. For e.g. one could just record the bridge differential voltage and demodulate it on a computer, to see if the problem was within the lock-in. This was done for various drive voltages and for various resistors. But the observed spectrum was still roughly the same, with a much steeper behavior then $f^{-0.5}$. This narrowed down the problem to the most unlikely of places- the amplifier. It would probably be worth trying the experiment with various other instrumentation amplifiers(like AD8229 or INA103).
- Another possible reason could be the lack of sufficient shielding. All the authors who have reported results on conduction fluctuations have described elaborate schemes to isolate the experiment from various external sources of noise. But, we have made no such attempts(see [8], [10], [14] for some shielding schemes).

In decreasing order of likelihood, the experimental setup being incorrect would be the most likely reason and the amplifier being faulty would be the least.

3.2.7 The cross correlation method

This is another method of extracting excess noise that we explored(see [13]) the idea is simple- if we pass the desired signal through two sets of identical electronics and calculate

the cross correlation spectrum of the resultant two identically conditioned signal we should get rid of the uncorrelated noise due to background electronics whereas the correlated noise would appear at the final output. The advantage of this method is that one can go below the background noise by averaging for sufficiently long amounts of time or ensembling averaging the obtained spectrum. Simulations were performed to test this idea[6] and this idea was also tested experimentally. The two outputs were cross correlated on MATLAB and then their cross power spectrum was plotted. The experimental schematic and final spectrum and a straight line fit for it is shown in a Figure-23 and Figure-24

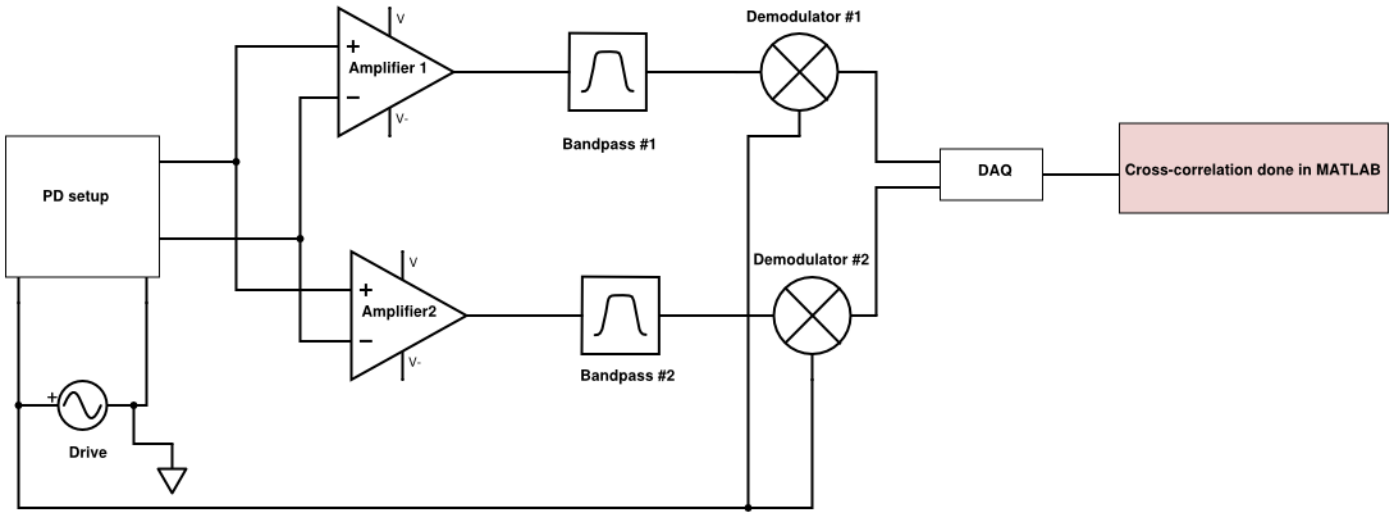

Figure 23: A schematic of the cross correlation method

A much better estimate of -1.63(that is the amplitude spectrum is $\propto f^{-0.8}$) was obtained but its still not in agreement with literature, but the estimate is much better. This method will be employed for photodiode noise measurements along with the $0-90$ subtraction technique described in the sections above.

3.3 Possible Alternate methods

We describe a method which was used in the analysis of crackling noise, which could as well be used to analyze resistor noise [4]. We had concluded that the net differential voltage seen across the bridge would be:

$$\Delta V = (\alpha(a_0 + a_2 \cos(2\omega_0 t) g(t) + i_{th}) R_0 \tag{15}$$

Here we have assumed perfect matching within all the resistors. $i_{th}(t)$ as before, represents the thermal noise current. Squaring both sides, we obtain the power time series of the spectrum.

$$\Delta V^2 = {i_{th}}^2 + \alpha g(t)^2 (a_0 + a_2 \cos(2\omega_0 t)^2 + 2 i_{th}(t)(a_0 + a_2 \cos(2\omega_0 t)) g(t) \tag{16}$$

[6] see Appendix E for the results of the simulations performed

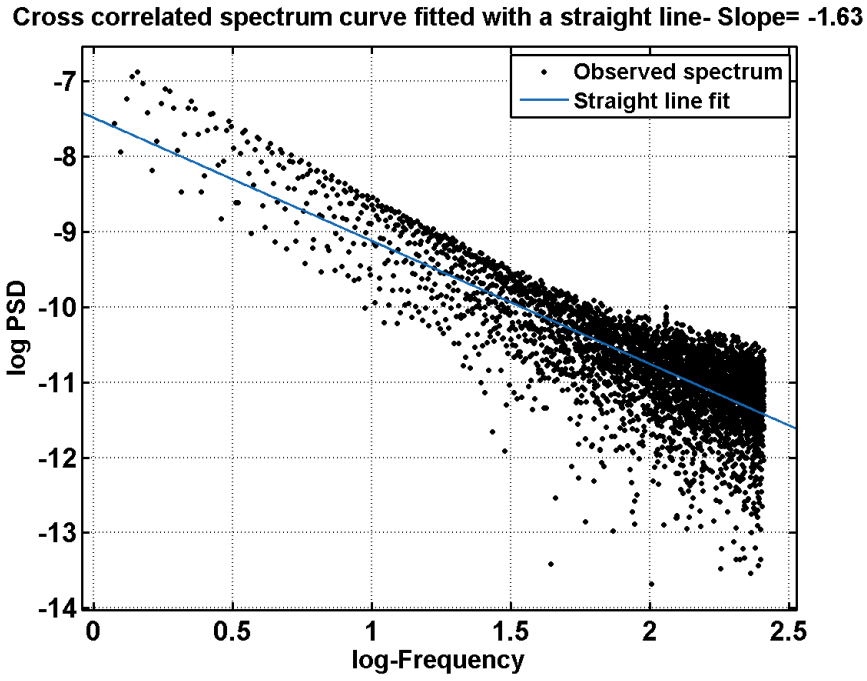

Figure 24: Straight-line fit for the obtained result of cross correlation method

We now take an ensemble average on both sides, this would give us

$$\langle \Delta V^2 \rangle = \langle i_{th}^2 \rangle + \langle (\alpha g(t))^2 \rangle (a_0 + a_2 \cos(2\omega_0 t))^2 + \langle 2 i_{th} \rangle (t)(a_0 + a_2 \cos(2\omega_0 t)) \langle g(t) \rangle \quad (17)$$

Assuming that all the stochastic process like $i_{th}(t), g(t)$ are zero mean processes. This would then result to

$$\begin{aligned} \langle \Delta V^2 \rangle &= \langle i_{th}^2 \rangle + \langle (\alpha g(t))^2 \rangle (a_0 + a_2 \cos(2\omega_0 t))^2 \\ &= \langle i_{th}^2 \rangle + \langle (\alpha g(t))^2 \rangle ({a_0}^2 + (a_2 \cos(2\omega_0 t))^2 + 2 a_0 a_2 \cos(2\omega_0 t) \langle (\alpha g(t))^2 \rangle \end{aligned} \quad (18)$$

By taking a Fourier transform of this power time series and then looking at value at $2\omega_0$.

$$\tilde{F}(2\omega_0) = 2 a_0 a_2 \langle (\alpha g(t))^2 \rangle \quad (19)$$

That is we obtain the total power of the random underlying stochastic process. The power time series can be additionally demodulated and then averaged for long times to obtain this value. Since we are measuring value of a signal at precisely one frequency i.e. at $2\omega_0$ we can now expect dig deeper below the Johnson by averaging for sufficiently long times and obtain this value. We bandpass(as we might want to analyze in a specific band) the power time series and take its ensemble average and then demodulate to get the total power contained.

4 Photodiode Noise setup

We now describe our the photodiode noise measurement experiment. The data analysis technique remains more or less identical to the one for resistor noise measurement. We then move onto describing our setup with special attention to how the laser was stabilized.

4.1 Basic Model

The excess resistor noise was attributed to material defects, similarly we model fluctuations in photodiodes by a fluctuating quantum efficiency, intrinsic to the photodiode just like resistors material defects. We could also model this as a noisy current source inside the photodiode, though this attempt was unsuccessful for the case of resistors but for active devices this might work. So our approach would be to inspect noise at both the fundamental harmonic as well as the second harmonic. Such a search would tell us a lot about the origin of the noise and also conclusively tell us which model is more suitable for modeling phototdiode noise. There have been few reports on photodiode noise measurements(see [18], [19]). We would like to characterize the excess noise spectrum with respect all the involved experimental parameters.

4.2 The experimetal setup

Figure [25] shows a rather oversimplified schematic of the experimental setup. It consists of a laser- the source, a accousto-optic modulator- this stabilizes the power fluctuations going to the photodiodes(these two are clubbed into the schematic), a pre-mode cleaner- its an optical cavity to suppress all spatial fluctuations which could lead to undesirable effects like pointing fluctuations which due to non-homogeneity of photodetector surface this could appear as a excess noise. Since frequency is not really a concern for our analysis, we lock the cavity so as to track the laser and make no special efforts to particularly stabilise the frequency itself. The intensity fluctuations are suppressed by taking the common mode of both the photodiodes and feeding it back to the AOM which stabilizes the power fluctuations.

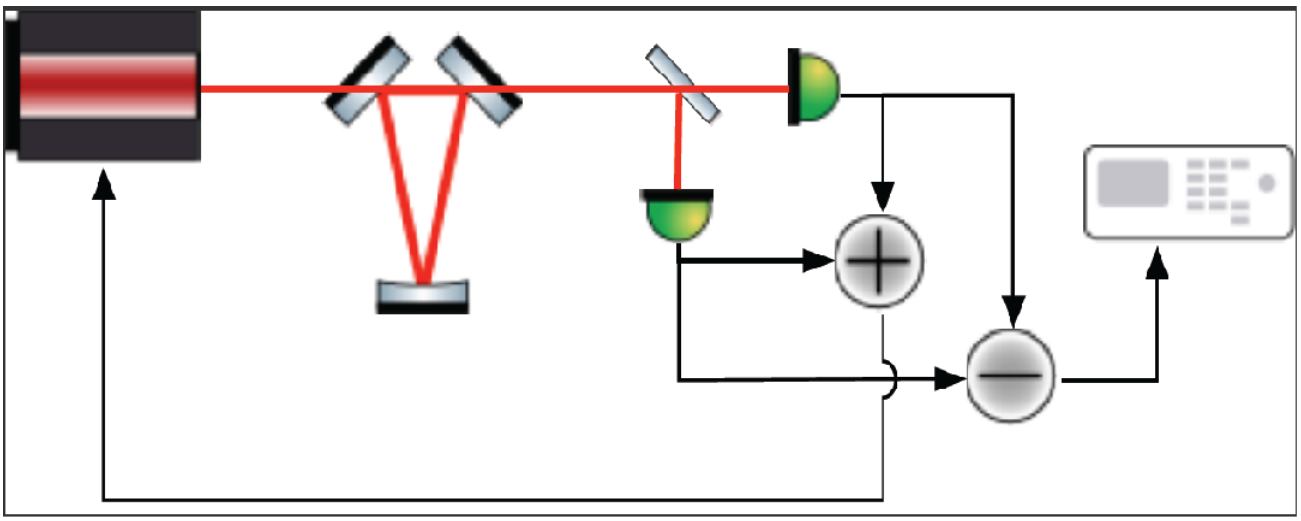

Figure 25: A simple schematic of the photodiode noise measurement setup

4.3 Laser Stabilization

4.3.1 Locking the cavity to the laser

The Pre-Mode Cleaner(PMC) is a Fabry-Perot cavity used to suppress higher order spatial modes. It also helps suppress effects like pointing fluctuations. The standard method used to lock a laser to relatively more stable cavity is the PDH(Pound-Drever-Hall) technique[7]). In this experiment we do not implement the exact PDH technique but a similar technique which produces a analogous error signal. We start by describing a generic feedback control and how PDH technique overcomes the challenges posed by such a method. In a generic method one would look at the reflection port of a cavity, which would have zero power output at resonance and if the laser changes its frequency by a small amount some power would leak out and this could be used to feedback to stabilize the laser. A schematic is shown below for this in Figure-26. There are few disadvantages to such a scheme, for e.g the photodiode

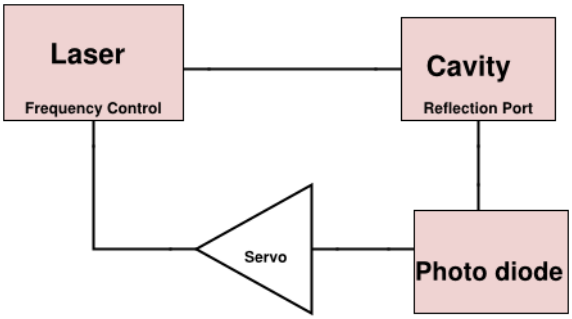

Figure 26: A simple schematic for locking the fluctuating laser to a stable cavity

at the reflection port has no way of knowing which side of the resonance is the laser at because the resonance curve for a cavity is symmetric about the resonance frequency. So if the laser frequency drifts the feedback circuitry has no know way of knowing which side of the resonance the laser is.

We describe the scheme below by which we locked the cavity to track the laser frequency.In our implementation we first dither the PZT actuator on the cavity and record the output of one of its transmission ports. The dither applied induces side bands in the the transmitted field and when one measures output power, this would have a component at drive frequency which when demodulated gives the error signal which can be fed back to the cavity. This leads to the cavity tracking the frequency of the laser. The schematic for the same is given below in figure [27] The math is described below. It is similar to how PDH scheme is analyzed. We know that in any optical cavity, the transmittance of a cavity is a function of the round trip phase and it appears as a complex exponential(that is it appears as $e^{i\delta}$, where δ is the round trip phase)(see [20] for a derivation of transmittance in a simple Fabry-Perot cavity). let the transmittance through the sensing port be $t(e^{i\delta})$, that is some function of $e^{i\delta}$, so this derivation works for any optical cavity as the dependence on round trip phase must occur in the form of $e^{i\delta}$. Now, from theory for Fabry-Perot cavities we know that $\delta = \frac{\omega L \beta}{c}$ Where δ is the round trip phase, L is the effective length of the cavity, ω is the frequency of incident light, c is the speed of light in the medium and β is some proportionality constant(which

[7]for a elegant description of the PDH technique see [30], [31]

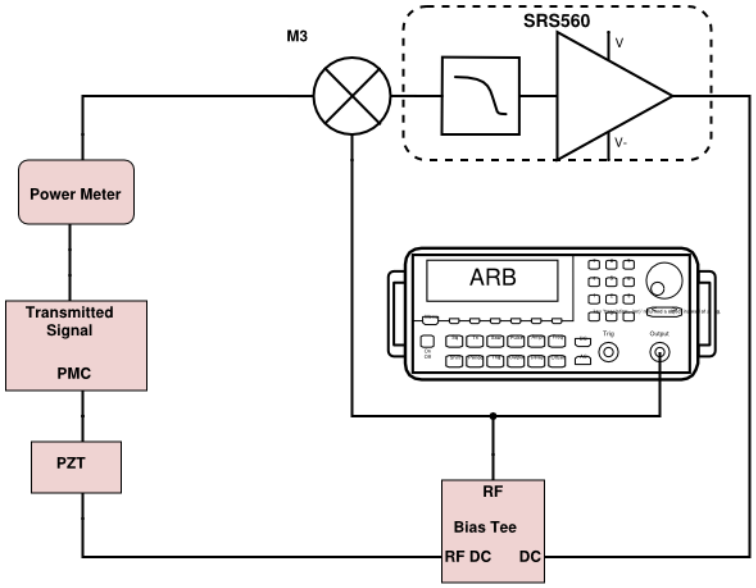

Figure 27: The schematic used for locking the cavity to the laser

would generally just be a number). By applying a dither to the PZT actuator we dither the effective length of the cavity this would imply the complex transmittance is changing as the dither is applied. Now, one do the following math:

$$t(\Delta L) = t(e^{i\frac{\beta\omega(L+\Delta L)}{c}}) \tag{20}$$

WhereΔL is the change in length due to the applied dither. Assuming a sinusoidal dither would mean that

$$\Delta L = l_0 \sin \Omega t \tag{21}$$

Where l_0 is some constant. The transmittance can now be expanded and manipulated as follows(let β/c be a constant κ):

$$\begin{aligned} t(\Delta L) &= t(e^{i\kappa\omega(L+l_0 \sin \Omega t)}) && (22)\\ &= t(e^{i\kappa\omega L} e^{i\kappa\omega l_0 \sin \Omega t}) && (23) \end{aligned}$$

$e^{i\kappa\omega L} = 1$, because at resonance length round trip phase must be integral multiple of 2π, let at resonance the transmittance through the sensing port be $t(atresonance) = t_0$. This would be when the cavity's length is perfect for resonates with the incoming field. Based on this we can write:

$$t(\omega) = t(e^{i\kappa\omega l_0 \sin \Omega t}) \tag{24}$$

This is the transmittance seen by a incident light wave at frequency ω with the dither applied. We can now expand the exponential sine in terms of its power series and for small dither we can truncate the series and keep only the first order terms.

$$e^{i\kappa l_0 \sin \Omega t} = 1 + i\kappa l_0 \sin \Omega t \tag{25}$$

Plugging this into the equation for transmittance we get-

$$t(\omega) = t(1 + i\kappa l_0 \sin \Omega t) \tag{26}$$

The meaning of the first term is a bit subtle- when expanding in terms of ω the 1 comes when $\omega = 0$, but a field with zero frequency would always resonate with this cavity (as its round trip phase would always be zero) and hence it can be equated to t_0.Taylor expanding this about ω we get

$$t(\omega) = t_0 + \frac{dt}{d\omega} i\kappa l_0 (\sin \Omega t) \tag{27}$$

when the length is being dithered around the resonance the transmittance for a light of frequency ω is:

$$t_0 + i\alpha \sin \Omega t \frac{dt}{d\omega} \tag{28}$$

where α just the product of all the other constants, in the equation. The transmitted amplitude for a electric field with equation $E_i(t) = E_0 e^{i \sin \omega t}$ would be

$$E_t(t) = E_i(t) \times (t_0 + i\alpha \sin \Omega t \frac{dt}{d\omega}) \tag{29}$$

$$= E_0 e^{i\omega t} (t_0 + i\alpha \sin \Omega t \frac{dt}{d\omega}) \tag{30}$$

Expressing $\sin \Omega t$ in terms of complex exponential we see that the transmitted amplitude is actually a sum of 3 frequencies- carrier at ω and two side-bands at $\omega - \Omega$ and $\omega + \Omega$. The beating of these side bands with the carrier is what reveals the side of resonance the system is on. Power of transmitted beam which is $P_t = E_t E_t^*$

$$P_t = |E_0 t_0|^2 + i\alpha \sin \Omega t (t_0 \frac{dt}{d\omega}^* - t_0{}^* \frac{dt}{d\omega}) + 2\Omega term \tag{31}$$

When demodulated we pick out the term attached to $\sin \Omega t$ which tells which side of resonance we are on. This would be a purely imaginary, but its absolute value will be a odd around resonance. That is the error signal coming from the output of the final low pass filter would be:

$$\epsilon = \alpha Im(t_0 \frac{dt}{d\omega}^* - t_0{}^* \frac{dt}{d\omega}) \tag{32}$$

In the region near resonance this would be linear and this signal can be then fed back to the PZT actuator, to make it track and stay locked with lasers frequency, similar to analysis in PDH. The final schematic adopted is given below in Figure-28.

4.3.2 Suppressing lasers intensity fluctuations

Laser's intensity fluctuations were suppressed using a AOM. AOM are acousto-optic devices which are based on the concept on Brillouin scattering of light(see [20], [21] for a detailed description of this effect). This results in a part of its power being diffracted at another frequency. The power in the secondary diffracted beam depends on the power in the acoustic waves which interact with the incident light wave. So by controlling the in power going into the AOM we control the power in the secondary diffracted wave and hence the power in the carrier wave. We measure the intensity of light coming through the PMC and then feed it back to control the power going into the AOM effectively stabilizing the power going into our experiment. The schematic for this control is in Figure-29.

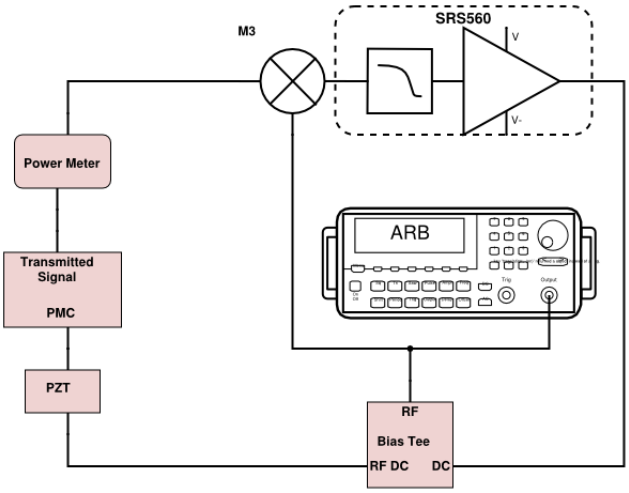

Figure 28: Cavity locking schematic

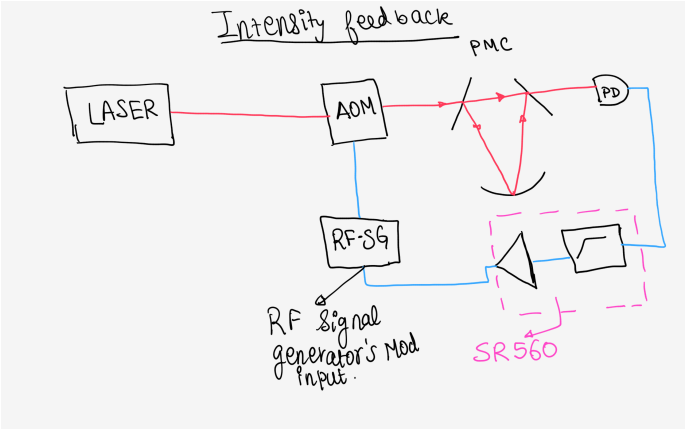

Figure 29: Laser intensity suppression schematic

5 Design and implementation of feedback loops

5.1 Frequency feedback loop- Filter design

The exact schematic of frequency stabilization was described in a previous section, here we describe the filter designed for it. The filter intended was a simple low pass filter with a cutoff at around 10Hz. The gain required was measured to be 200. A further complication was introduced because of the piezo driver which introduced a pole at 8Hz. For this purpose a zero was introduced at 500Hz, to flatten the frequency response beyond 500Hz, as a 2nd order low pass filter is very likely unstable at such a high gain. The schematic for the circuit is given in figure 30. The piezo driver is modeled as simple one pole system at 8Hz. The

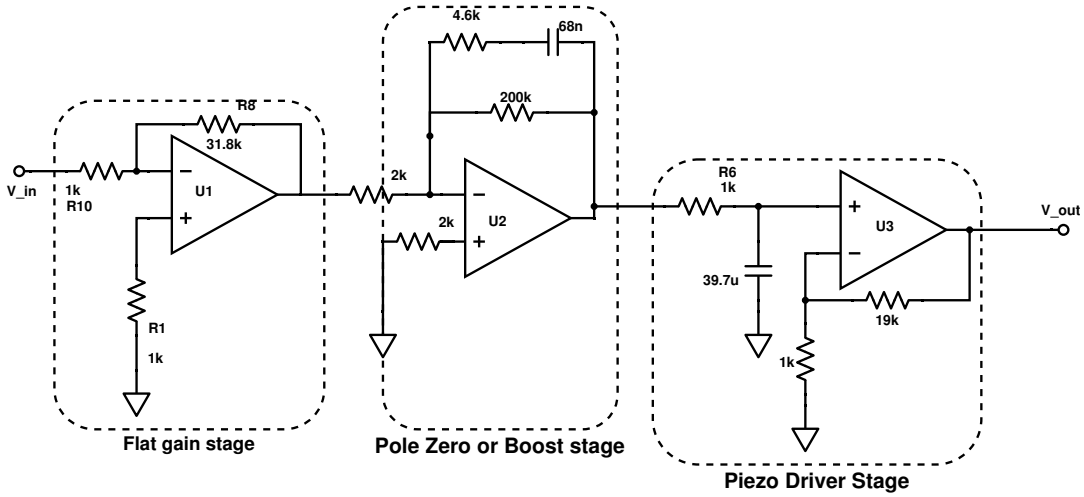

Figure 30: Circuit schematic for frequency feedback, the stages consist of one flat gain stage, a pole-zero stage and piezo has been modeled as a single pole system.

cicuit was simulated on LISO and after a few iterations we were able to get the cavity locked to the laser for sufficient amount of time. The open loop gain for this feedback schematic is presented in figure 31.

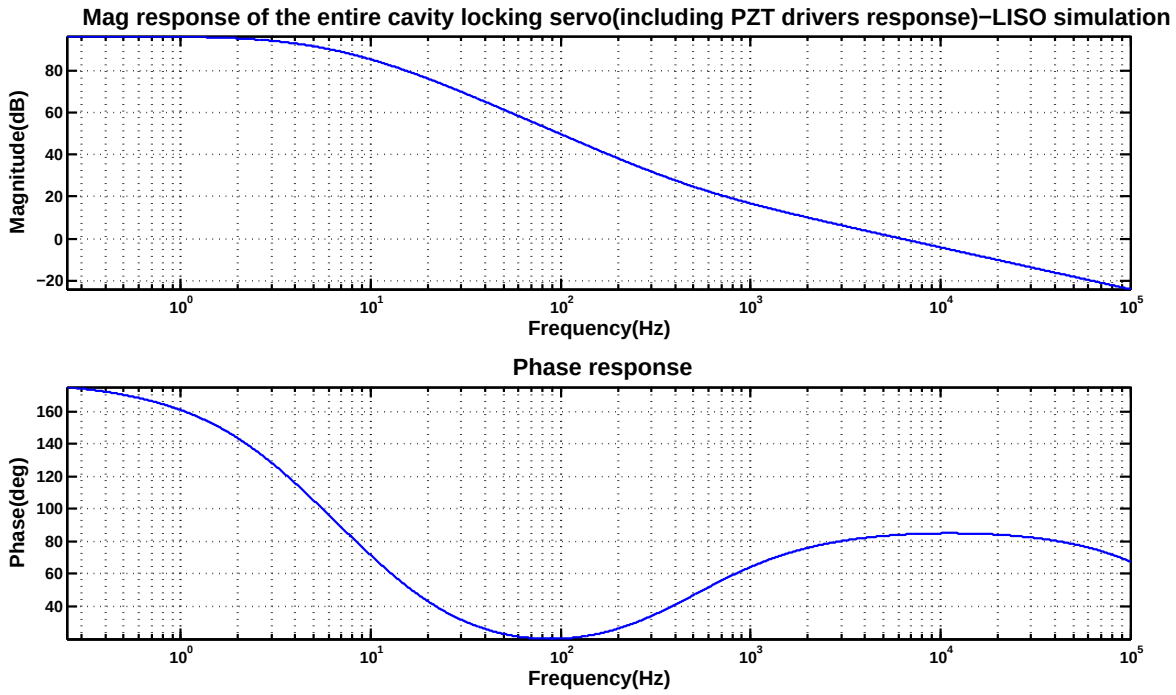

Figure 31: Open loop gain of the feedback schematic designed-The features are exactly as predicted, a steep slope from the two poles and a flattening effect by the zero after 500Hz, this combined with a flat gain stage pushes the UGF to almost 7kHz, which is more than sufficient for our purpose.

Once, this filter was realised the laser was locked to test its efficiency and the time for which the cavity tracked the laser. The cavity stayed locked for over extended periods of time.

5.2 Intensity suppression feedback schematic

The design of the intensity feedback servo turned out to be a bit more subtle. Firstly, one cannot design simple low pass filter with a high gain for this, because then it would suppress power at DC as well, which not desirable. If one indeed uses this schematic, one would have to add a quiet reference in the feedback servo. To avoid such hassle, we decided to suppress fluctuation only in the desired band of interest(1Hz- 1kHz). One has to also decide, how much suppression is exactly needed for such a feedback servo. The free running laser noise, which is expressed as RIN(relative intensity noise) was measured to be $10^{-4}\sqrt{Hz}$ at 1Hz. Since, the signal of concern is the differential signal of PDs, the differential amplifier which will be incorporated in the readout circuit will also provide some suppression to the common mode noise. The intensity suppression of the feedback should be designed so that, when combined with that of the differential amplifier used, it should reduce the common mode noise of the system below the differential noise which is being measured. Another subtlety that we encountered was that, one has to also take into account the fact that the RF function generator, RF power amplifiers, AOM have their own transfer functions. The first step in designing the feedback would be to measure this frequency response of the remaining loop,

which constitutes the actuator. The transfer function of the remaining loop was measured using the voltage injection technique. The transfer function of the remaining actuator will also decide how much gain will be required for the the feedback filter to be designed. Figure 32 shows the measured open loop response of the actuator as a whole. The phase response

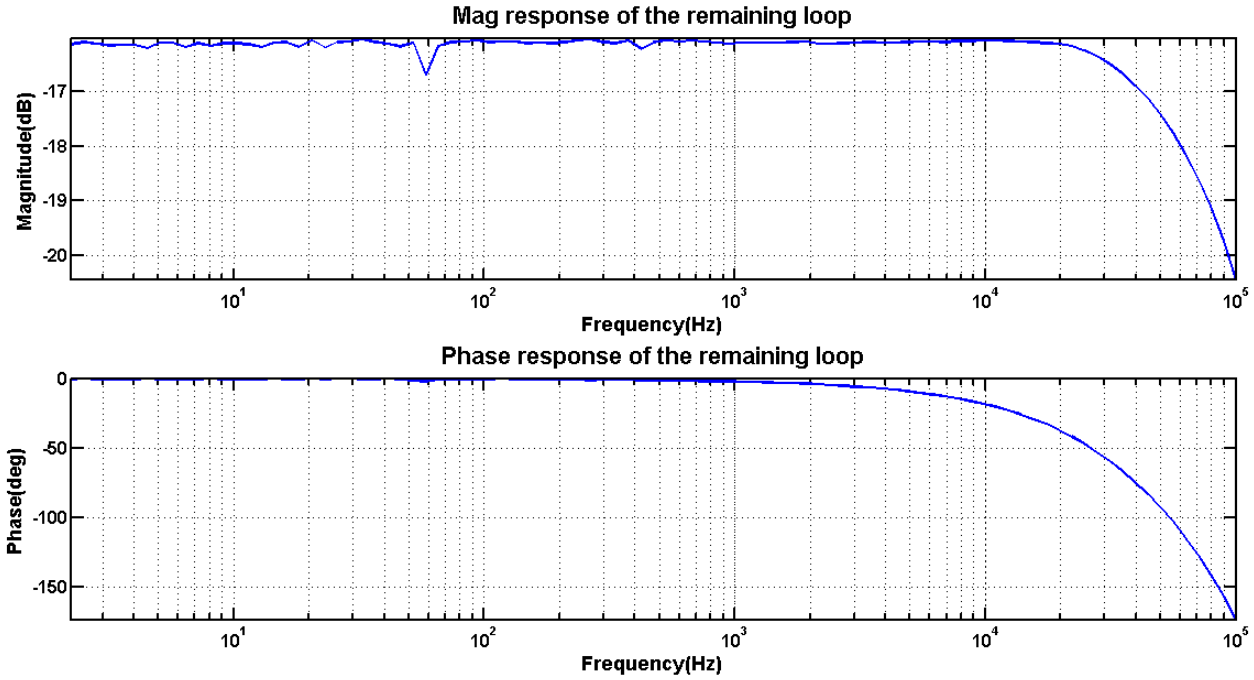

Figure 32: The open loop response of the actuator which consists of RF function generator, the AOM and the PDs

is zero till around 10kHz, it will not influence the phase of our servo in the frequency band of interest. The magnitude response indicates around -17dB of attenuation which will have to be accounted for when calculating parameters for the feedback servo.
We went on to analyze the free running laser noise of the laser, as this would provide us a estimate of the suppression we want. As mentioned before the RIN was measured to be $10^{-4}/\sqrt{Hz}$ at 1Hz. Figure 33 shows the measured RIN of the two PDS.

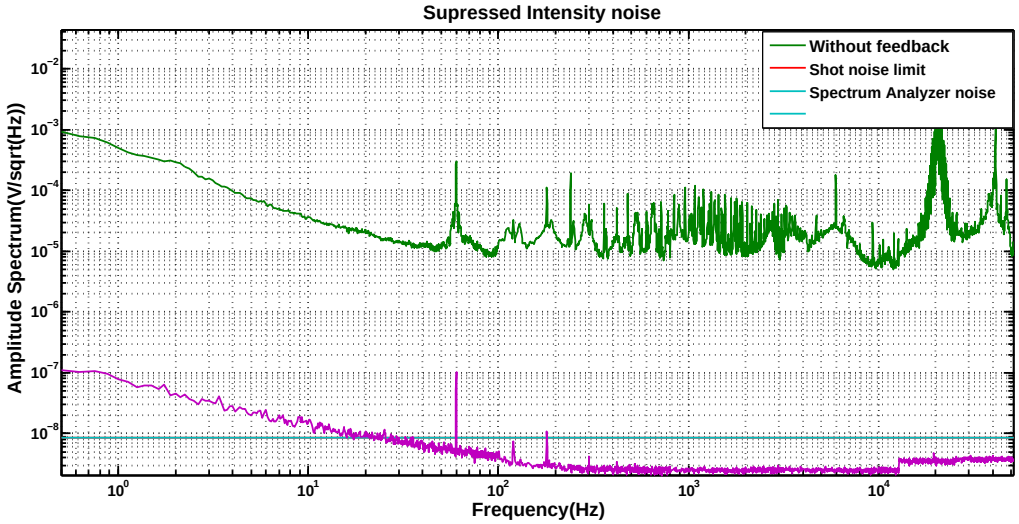

Figure 33: Free running laser noise, along with it the shot noise limit and the spectrum analyzer noise is displayed

We decided to start with a suppression of 100 in the bandwidth of interest(1Hz-1kHz), in the form of a simple first order band-pass filter. The bandpass filter and the resultant open loop gain of the feedback servo was simulated. We went on to calculate the open loop gain of the feedback servo using the voltage injection method. The results are presented in figures 34, 35.

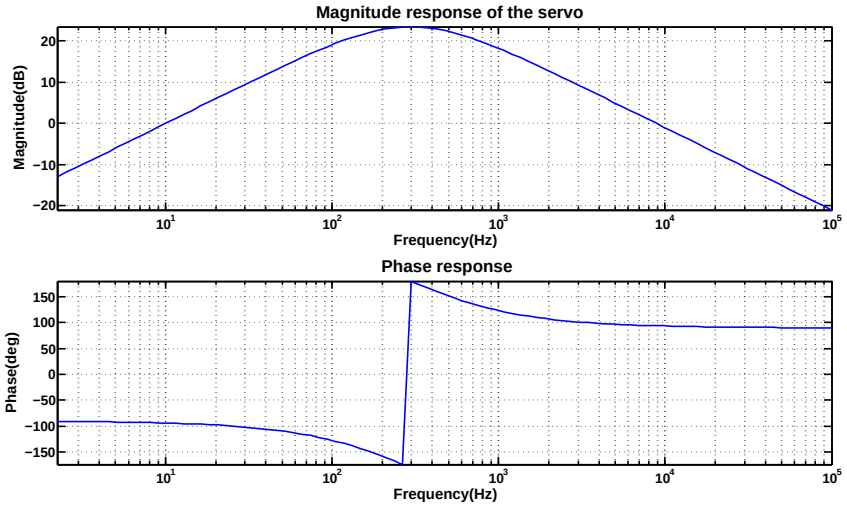

Figure 34: Filter designed for feedback to suppress intensity fluctuations is shown. The filter is a simple bandpass filter with required gain to suppress fluctuations in the band of the interest.

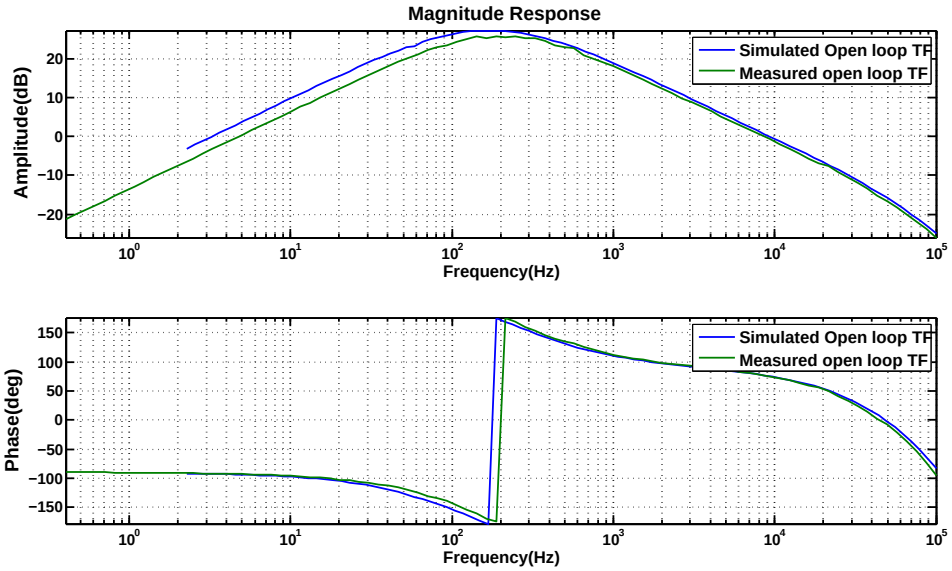

Figure 35: Figure shows the total open loop gain including the actuators response as compared to the simulated response. It is not hard to see that they are in good agreement.

We went to onto implement the servo and measure the PD's signal the result for the same is presented in figure 36

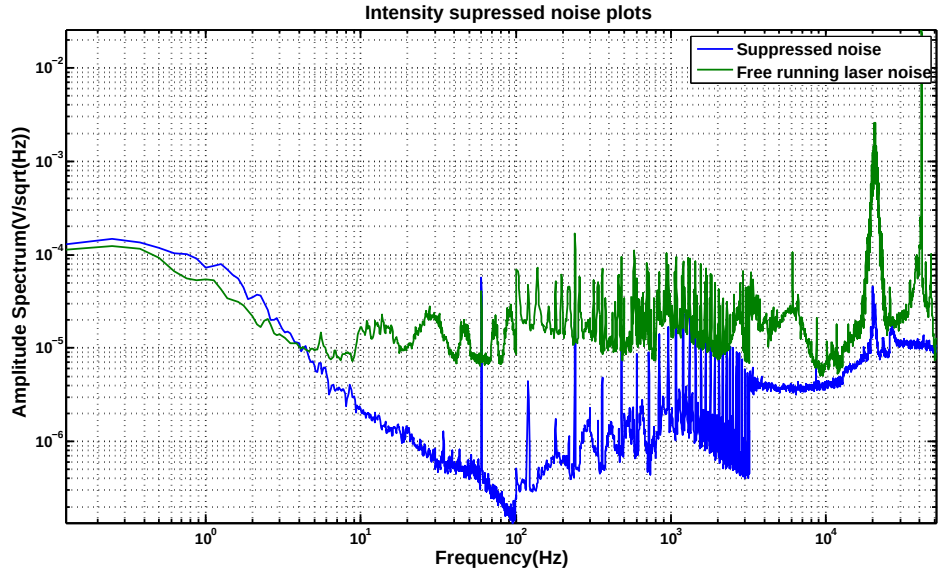

Figure 36: The suppression was as expected, 2 orders of magnitude in the region of interest(1Hz-1kHz). Since a lot of frequency ranges were spliced together to create this, the figure looks a bit discontinuous, but retains its essential features.

6 Future Work

Though we were able to finish majority of the implementation of project, we weren't able to acquire data and analyse it. Even before that is done, it would be necessary to check if the provided suppression is indeed sufficient to measure the differential signal of the PDs. For which we have created a small circuit consisting of a differential amplifier. Also, since we are going to use the heterodyne detection scheme, we will have to modulate the power going to the two PDs. This could be accomplished by injecting a sinusoidal signal in the feedback loop, with a amplitude calibrated to the actuators response. We calibrated actuators response way before we implemented the filter, but we were not able to combine it with the filter. The last part would then be to acquire data and possibly use one of the many techniques discussed here to extract the signal. It would be very interesting to measure excess noise as a function of various parameters like, amplitude of the sinusoidal signal, bias voltage, the type of PD etc.

Appendix

A Derivation of bridge voltage in terms of resistance fluctuations

Consider the figure [37], in which nodes are marked with their corresponding voltages. $V_a - V_b$

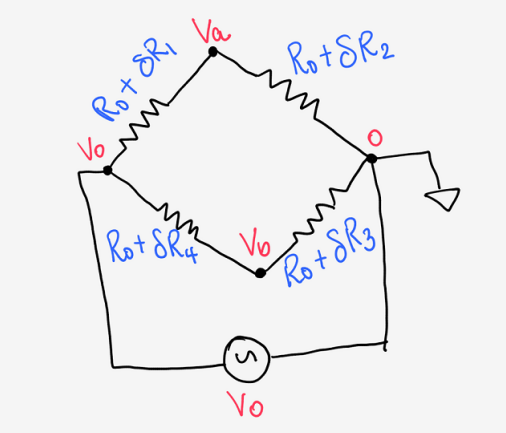

Figure 37: Nodal Diagram of the circuit

is what is required, we can write nodal equations at the nodes a and b which would look as follows:

$$\frac{V_a - V_0}{R_0 + \delta R_1} + \frac{V_a}{R_0 + \delta R_2} = 0 \tag{33}$$

$$\frac{V_b - V_0}{R_0 + \delta R_3} + \frac{V_b}{R_0 + \delta R_4} = 0 \tag{34}$$

These are reduced to simpler forms using the binomial expansion[8]

$$(1-\frac{\delta R_1}{R_0})(V_a-V_0)+V_a(1-\frac{\delta R_2}{R_0})=0 \tag{35}$$

$$\tag{36}$$

Expressing V_a in terms of V_0

$$V_a = \frac{V_0(1-\frac{\delta R_1}{R})}{2(1-\frac{\delta R_1+\delta R_2}{2R})} \tag{37}$$

$$V_a = \frac{V_0(1-\frac{\delta R_1}{R_0})(1+\frac{\delta R_1+\delta R_2}{2R_0})}{2} \tag{38}$$

Similarly V_b can also be expressed in a similar way in terms of V_0, δR_3 and δR_4

Now, $V_a - V_b$ would be, after neglecting second order terms

$$V_a - V_b = \frac{(\delta R_2+\delta R_3-\delta R_1-\delta R_4)V_0}{2R_0} \tag{39}$$

B Derivation of power spectra at the output of lock-in amplifier

Recall that the voltage fluctuations as measured across the bridge would be:

$$\Delta V(t) = \frac{i_0 \delta R(t)\sin\omega_0 t}{R_0} + \delta v_0 \tag{40}$$

δv_0 refers to the background noise. The fourier transform of this signal would be

$$\Delta\tilde{V}(\omega) = [\frac{i_0}{2j}(\tilde{\delta r}(\omega+\omega_0)+\tilde{\delta r}(\omega-\omega_0)+\tilde{\delta v_0}(\omega)] \tag{41}$$

The lock-in multiplies this by a pure sine wave at ω_0 with a phase difference of θ frequency and then multiplied by a low pass filter lets its transfer function be $H_l(\omega)$. The output of the lock-in would have a fourier transform of:

$$\Delta\tilde{V}_o(\omega) = \frac{H_l(\omega)}{2j}[(\delta(\omega-\omega_0)e^{j\theta}-\delta(\omega+\omega_0)e^{-j\theta}) * \Delta\tilde{V}(\omega) \tag{42}$$

The Fourier transform of a pure sine is a Dirac delta function and since its being multiplied in the time domain it would be convulated in the Fourier domain which is what the $*$ represents this is then low passed with a low pass filter $H_l(\omega)$. The power spectrum of this would be defined as $S_V(\omega) = \int_{-\infty}^{\infty}\Delta\tilde{V}_o(\omega)\Delta\tilde{V}_o(\omega)^* d\omega$. This can be evaluated and under the assumption that the low pass filter has its cutoff frequency less than ω_0 the desired result can be easily obtained.

C Additional plots

[8] $(1+n)^{-1} \approx 1-n$ for $n \ll 1$

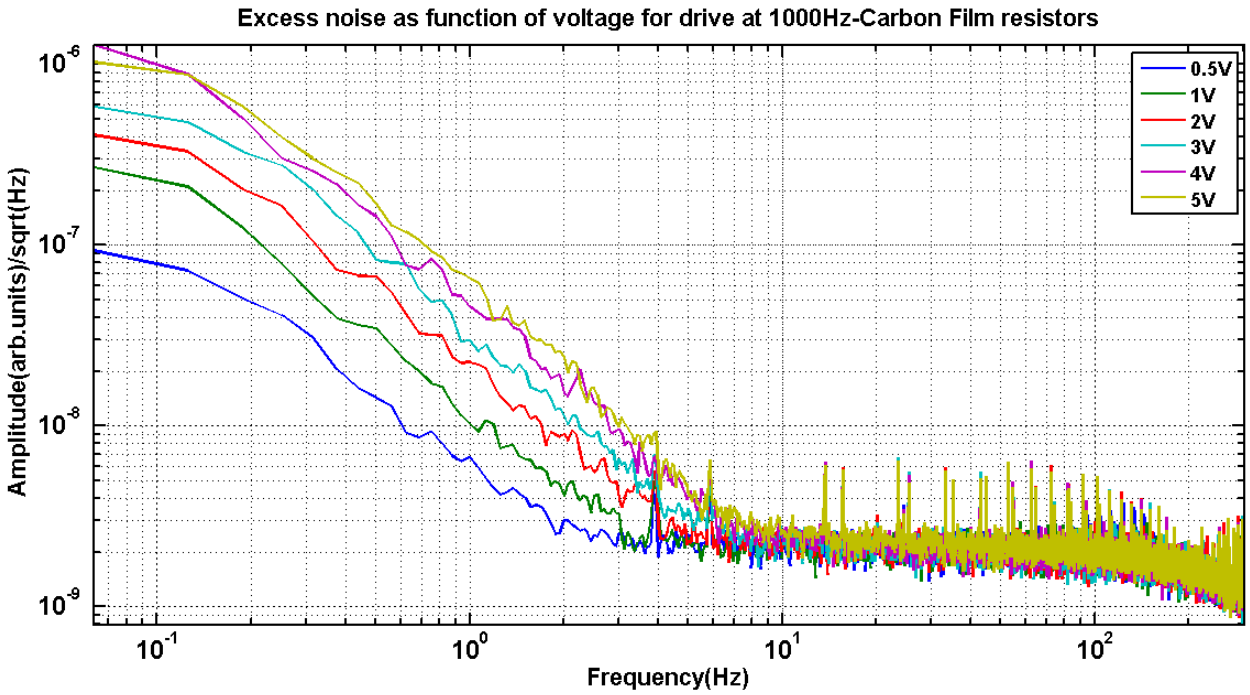

Figure 38: Excess noise spectrum as a function drive voltage(0.5V to 5V) for a drive frequency of 1000Hz

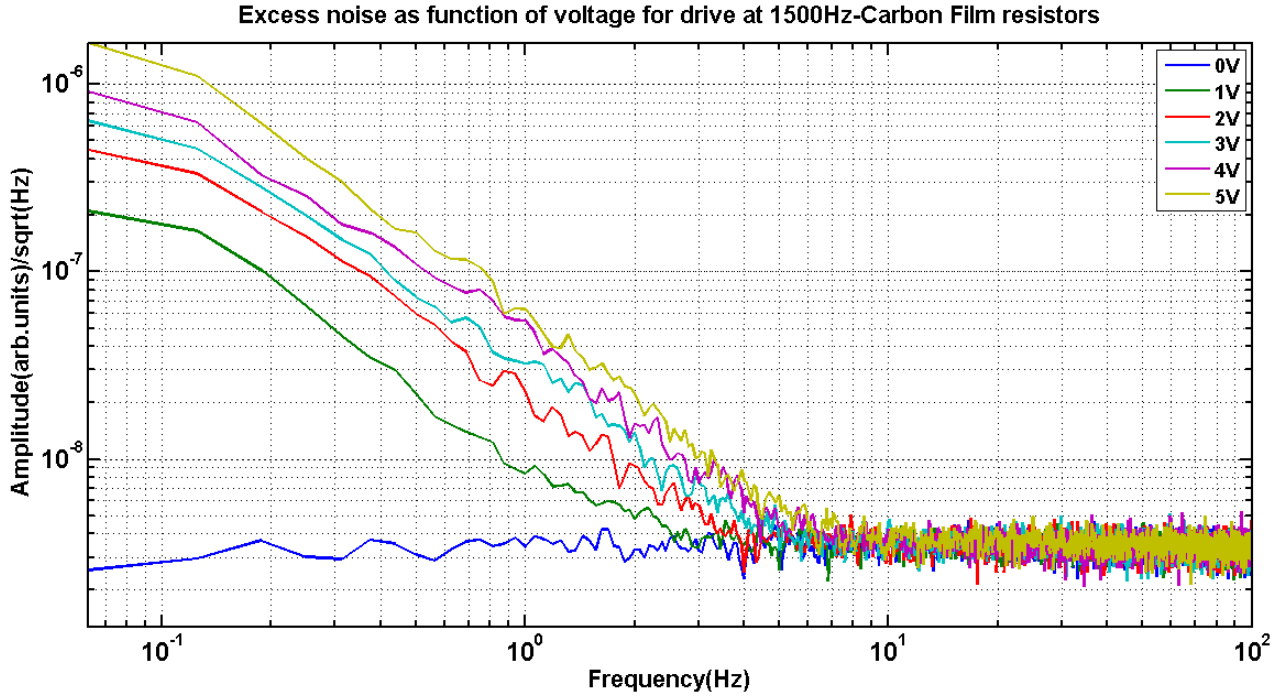

Figure 39: Excess noise spectrum as a function drive voltage(0.5V to 5V) for a drive frequency of 1500Hz

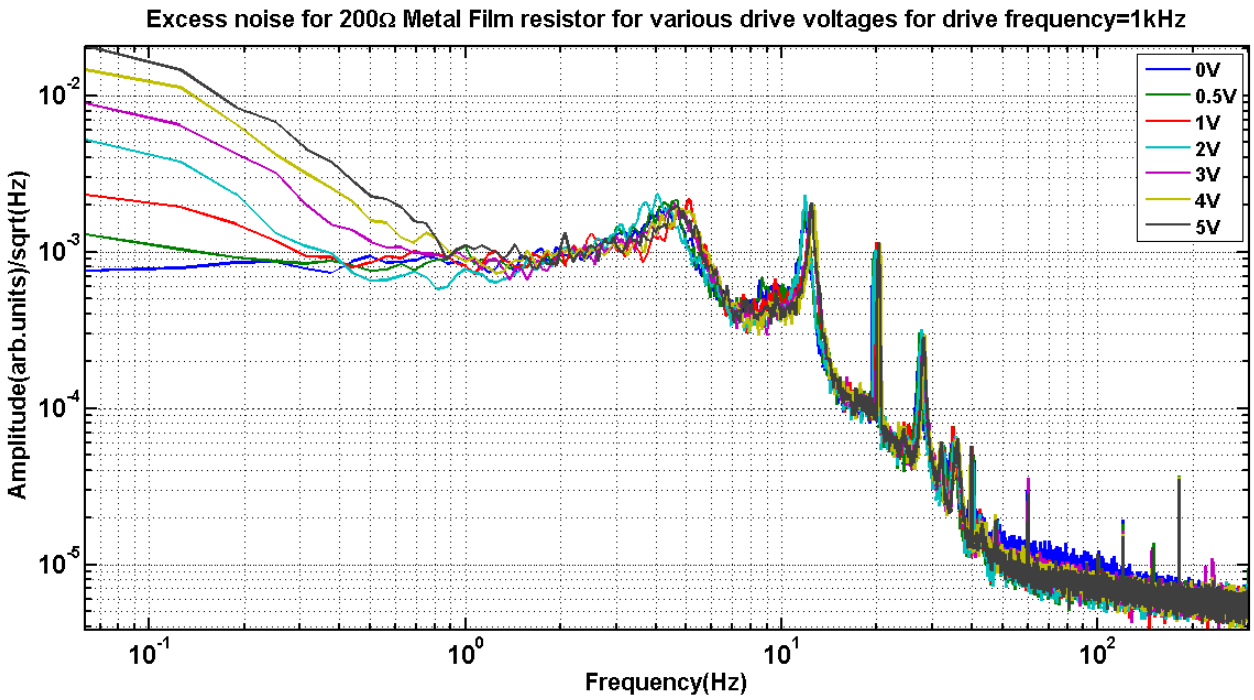

Figure 40: Excess voltage noise observed in 200Ω MF resistors as function of drive voltage for drive frequency of $1kHz$

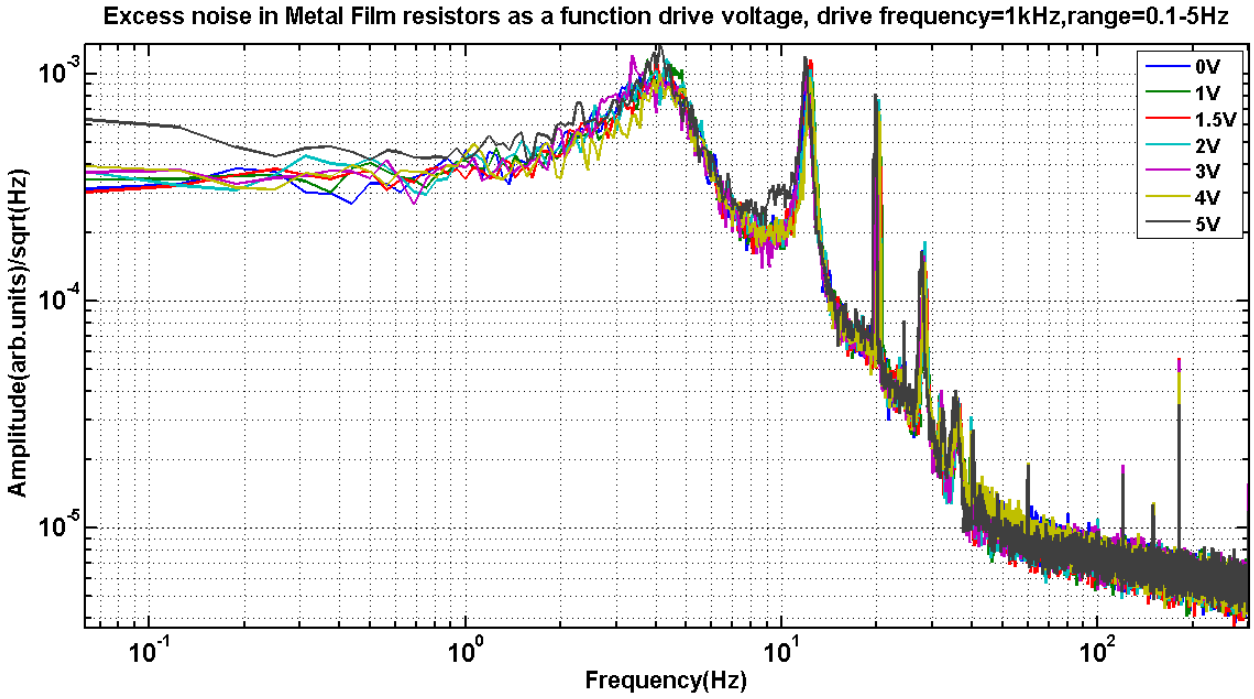

Figure 41: Excess noise spectrum for a $1.5k\Omega$ MF resistor, note the magnitude of noise whihch is roughly 2 orders of magnitude smaller than $1.5k\Omega$ CF resistor for identical drive conditions

D Noise plot of various instruments used

This section has the noise plots of the various instruments that were used. Figure 42 is the noise spectrum of the DAQ, Figure 43 is the noise spectrum of the amplifier used, it can be seen that the limiting noise is actually DAQ noise.

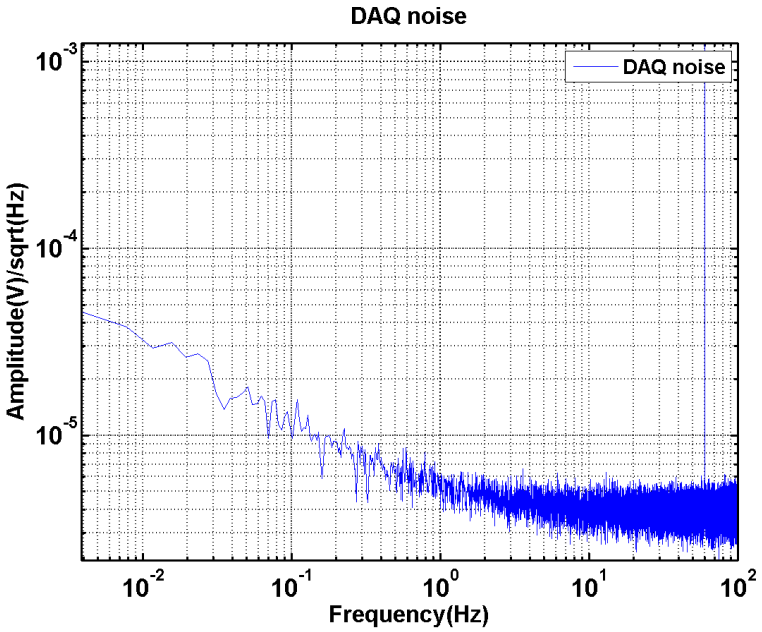

Figure 42: DAQ Noise

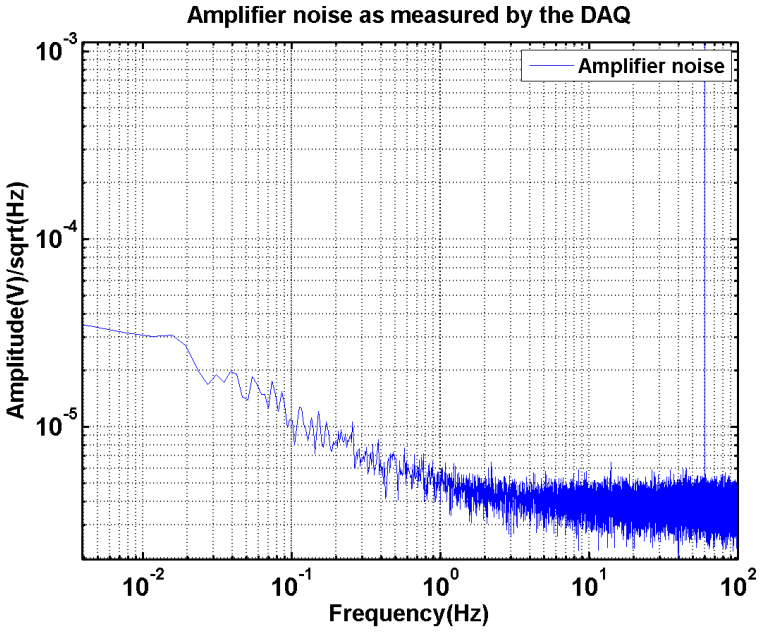

Figure 43: Amplifier noise as measured using the DAQ

E Simulations for the cross-correlation method

We present the results of simulations on the cross-correlation method. The following figures show the actual excess noise to be detected, the background noise level and the estimate as obtained from cross correlation method for various number of ensemble average of the obtained spectrum. The only thing to observe is how the estimation better by increasing the number of ensemble averages performed.

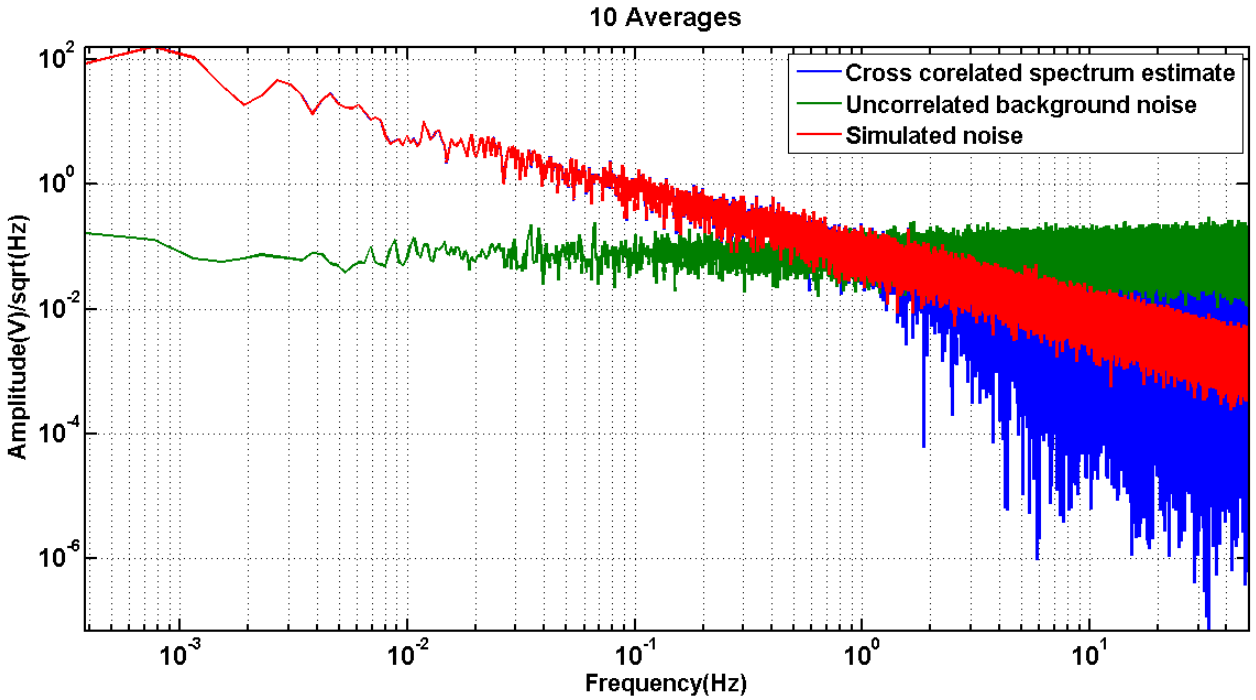

Figure 44: Ensembled averaged for 10 realizations of the spectrum

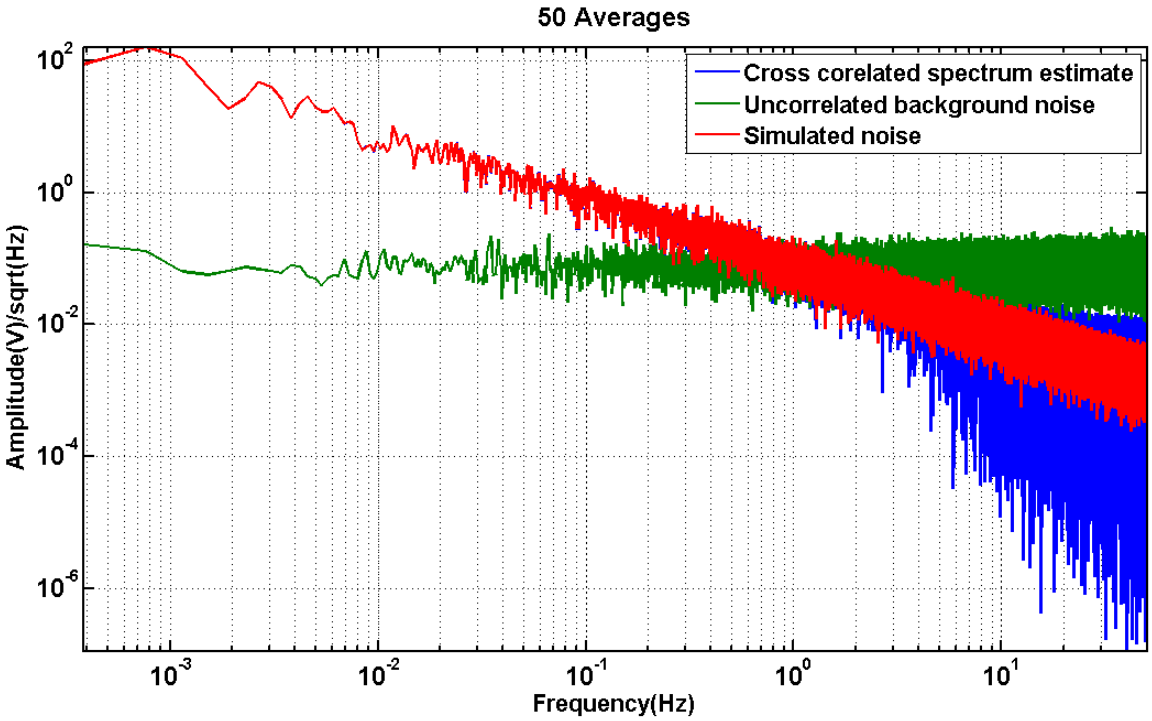

Figure 45: Ensembled averaged for 50 realizations of the spectrum

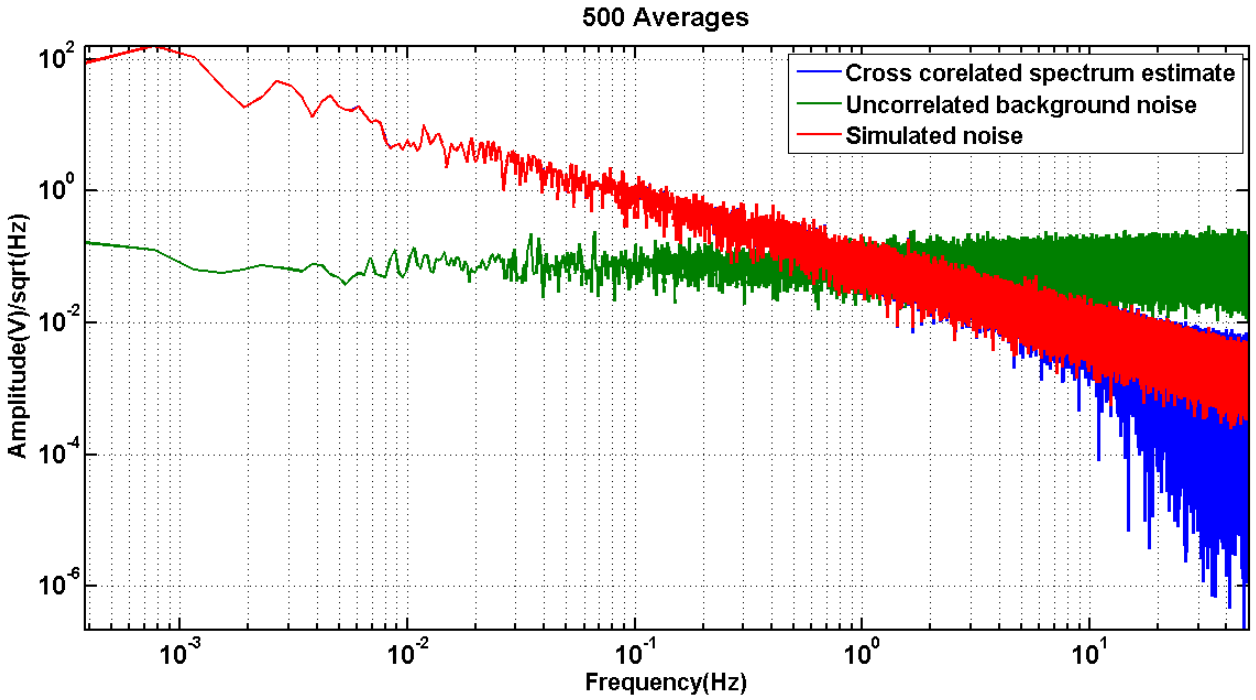

Figure 46: Ensembled averaged for 500 realizations of the spectrum

References

[1] Fredric Cleva, Jean-Pierre Coulon, Alain Brillet, Li-Wei Wei, *Laser power stabilization with a single high-power photodiode*

[2] Frank Seifert, *Resistor Current Noise Measurements* -LIGO-T0900200-v1

[3] Hristo Zhivomirov,*Pink Noise Generation with MATLAB Implementation*

[4] Eric Quintero, Eric Gustafson, Rana Adhikari *Experiment to Investigate Crackling Noise in Maraging Steel Blade Springs*

[5] Edoardo Milotti, *1/f noise: A pedagogical review.*

[6] F.N.Hooge, *1/f noise sources.* IEEE Transactions on Electronics Devices, Vol.41, No.11, November 1994

[7] S Demolder, MVandendriessche,A Van Claster, *The measuring of 1/f noise of thick and thin film resistors.* J.Phys.E:Sci. Instum., Vol. 13,1980

[8] John H.Scofield *ac method for measuring low-frequency resistance fluctuation spectra.* Rev.Sci. Instrum. 58(6), June 1987

[9] Eric Quintero, Eric Gustafson, Rana Adhikari *Experiment to investigate carackling noise in maraging steel blades.* LIGO-T1300465-v2

[10] Arindam Ghosh, Swastik Kar, Aveek Bid, A.K. Raychaudhari, *A setup for measurement of low frequency conductance fluctuations using digital signal processing techniques.* arXiv:cond-mat/0402130v1.

[11] Frederic Cleva, Jean-pierre Coulon, Alain Brillet, Li-wei wei, *Laser power stabilisation with a single high-power photodiode.*

[12] Frank Siefert, *Resistor Current Noise Measurements*, LIGO-T0900200-v1.

[13] S.Demolder, A.Van Calster, M.Vandendriessche *Current Noise in Thick and Thin Film Resistors.*

[14] J.Heefner, *Resistance noise measurement Summary,*LIGO-T070019-01-C.

[15] Patrick Barry and Steven Errede, *Measurement of 1/f Noise in Carbon Composition and Thick Film Resistors*, Senior thesis- University of Illinois at Urbana-Champaign, Fall 2014.

[16] Peter M. Marchetto, *1/f and Johnson-Nyquist Noise in metal-film and carbon resistors.*

[17] Walter C. Pflanzl, Ehrenfried Seebacher, *1/f Noise Temperature Behaviour of Poly Resistors*, 19th International Conference "Mixed Design of Integrated Circuits and Systems", May 24-26, 2012.

[18] O.Llopis, S. Azaizia, K.Saleh, A.Ali Slimane, A.Fernandez *Photodiode 1/f noise and other types of less known baseband noises in optical telecommunications devices.*

[19] Djati HANDOKO, Dong-Hyun KIM *1/f noise caracterstics of a photodiode signal under illumination by a linearly polarized diode laser* New physics: Sae Mulli(The Korean Physical Society), Volume 62, Number 5, 2012.

[20] Amon YAriv, Pochi Yeh *Photonics- Optical electronics in modern communications*Sixth edition, Oxford university press, 2007.

[21] Robert Boyd, *Non-linear optics*, Third edition.

[22] G. Q. Yu1, Z. Diao, J. F. Feng, H. Kurt, X. F. Han, J. M. D. Coey1 *1/f noise in MgO double barrier magnetic tunnel junctions*, Appl.Phys.Lett 98, 112504(2011).

[23] Hui Tian, Abbas El Gamal, *Analysis of 1/f noise in switched MOSFETs circuits*,IEEE Transactions on Circuits and SystemsII: Analog and Digital Signal Processing, VOL. 48, NO. 2, Feb 2001.

[24] http://www.ece.unm.edu/faculty/bsanthan/ece541/cycloex.pdf

[25] http://dsp-book.narod.ru/DSPMW/17.PDF

[26] William.A.Gardener, Lewis.E.Franks, *Characterization of cyclostationary random processes*,IEEE Transactions on Information Theory, VOL.IT-21, NO. 1, Jan 1975.

[27] *SR830-Users manual*,http://www.thinksrs.com/downloads/PDFs/Manuals/SR830m.pdf

[28] *SR830-Datasheet*, http://www.thinksrs.com/downloads/PDFs/Catalog/SR810830c.pdf

[29] John Bechhoefer, *Feedback for physicists: A tutorial essay on control*, Reviews of Modern physics, Vol.77, July 2005.

[30] Eric.D.Black, *A introduction to Pound-Drever-Hall laser frequency stabilization*

[31] Eric.D.Black *Notes on the Pound-Drever-Hall technique*, LIGO-T980045-00-D

[32] Jan Hendrik Põld, *Design, Implementation and Characterization of the Advanced LIGO 200WLaser System*